Interactive comment on "Glacial history of Inglefield Land, north Greenland from combined in-situ 10Be and 14C exposure dating" by Anne Sofie Søndergaard et al.

Yarrow Axford (Referee)
axford@northwestern.edu
Received and published: 29 June 2020

This paper presents new 10Be and in situ 14C constraints on the timing of early to middle Holocene deglaciation of Inglefield Land in northwest Greenland, and 14C ages from reworked organic materials that record a period in the middle to late Holocene when the Greenland Ice Sheet in the study area was smaller than present. The combination of 10Be and in situ 14C reveals extensive nuclide inheritance in the region, indicating past cold-based ice cover / mimimally erosive ice, especially on highlands. The paper thoughtfully integrates all data types to reconstruct the ice sheet margin history in an area where more data are badly needed. And I appreciate the review of prior work to piece together a broader picture of regional glacial history. Altogether, the paper documents some regional coherence as well as complex spatial variations in the timing of glacier margin changes, and those patterns should ultimately – in concert with future work to flesh out the paleoclimate and/or glacial history in even greater detail – help our community understand key aspects of ice sheet dynamics. I enthusiastically recommend this study for publication after minor revisions. It takes a thorough, multimethod approach to fleshing out the glacial history of a poorly known sector of the Greenland Ice Sheet.

My most significant suggestion is to better describe the morphostratigraphic contexts of the 14C-dated organic materials, and in the case of the wood fragments the rationale for inferring that they derive from inboard of the modern ice sheet margin. I think the link between minimum ice sheet extent in the middle Holocene and the inferred driver of ocean climate (vs. atmospheric), could also be further considered and further justified.
The above has been addressed in the following individual comments and changes have been incorporated into the manuscript.

Detailed comments:

Methods and Tables 1/2: What were the lithologies of the boulders sampled for 10Be? Were they consistent with the local bedrock (or likely far-traveled from inland under the ice sheet)?

Answer: We have added a couple of lines in the Methods section about the lithology and our interpretation of transport distance.

"The lithology of boulders sampled were all granite or gneiss, matching the lithology in and around Inglefield Land, but due to the placement on bedrock and moraines we assume the boulders to be transported some distance before deposition."

(And in Results, any pattern of different lithologies among the oldest vs youngest 10Be ages, ie degree of inheritance?) Or is everything uniformly granitoid/ gneiss with local vs exotic provenance impossible to pin down?

Answer: Everything is uniformly granitoid/gneiss. We have looked into possible patterns between the lithology and inheritance, especially Feldspar (Al) content in the samples, but there is no clear pattern between ages and lithology. We have added a comment in the results section (4.1) about this.

Please describe further the morphostratigraphic contexts of the dated wood fragments. Were they exposed on the surface of the meltwater plain, coming out in meltwater right at the ice front, or found buried in an outcrop of river deposits?

Answer: The wood fragments were collected together with samples presented in recent studies concerning the Hiawatha Impact crater (Kjær et al., 2018; Garde et al., 2020). We have added more information on the sample site in the methods section 3.2.

Any evidence for the species of the "wood"?

Answer: It has not been possible to identify the dated wood found in front of the Hiawatha Glacier.

It would be useful to include any information that rules out or argues against these materials having been exhumed by water or wind from a nearby soil (instead of excavated by ice inboard of the present-day ice sheet margin, as is inferred). This possibility should be discussed in the Results and/or Discussion as well.

Answer: We have commented on this in the results section 4.2, where we argue for our interpretation of the wood fragments having originated from underneath the glacier.

"As the wood fragments were retrieved right in front of the Hiawatha Glacier, the wood fragments are more likely to have originated from underneath the glacier than being transported from a nearby soil to the sample site by wind or water. We therefore believe these ages to constrain a time when the glacier was smaller than its present-day extent."

There is a brief description of context for the 14C-dated molluscs (on and within diamicts), but it appears in Results and I suggest putting this fundamental sampling information in Methods.

Answer: This information has been moved so it now appears for the first time in the methods section.

Line 273: "the ice margin reached its present-day extent at Delta Sø c. 10.1 ka" The age of 10.1 ka is actually the basal age from Wax Lips Lake, which is indeed the best constraint on when ice in that region reached its modern extent because WLL is situated only _2 km from the modern ice margin (McFarlin et al 2018 PNAS, discussed in Axford et al. 2019). Suggest changing "Delta So" in this sentence to "Wax Lips Lake" and citing McFarlin (and add WLL to Fig 8a if needed).

Answer: The sentence and reference have been changed as suggested and the location of Wax Lips Lake has been added to figure 8a.

Line 284: "Farther north in the Thule area and around Qaanaaq, mosses from a local ice cap and subfossil plants from the GrIS show a smaller ice extent before c. 3.3 cal. ka BP (Farnsworth et al., 2018; Axford et al., 2019: : :" Just a note that Axford et al. also find the North Ice Cap was smaller than present for most of the Holocene, as reflected in your Fig 8c, and that seems to contrast with the wording here.

Answer: The 3.3 cal. ka BP is linked to the study around Qaanaaq - we have re-phrased the sentence for clarity so it now reads: Farther north, mosses from a local ice cap and subfossil plants from the GrIS show a smaller than present-day ice extent before c. 3.3 cal. ka BP around Qaanaaq and throughout most of the Holocene until c. 1850 AD in the Thule area (Farnsworth et al., 2018; Axford et al., 2019; Søndergaard et al., 2019).

Line 299: I think it is debatable whether the early Holocene peak warmth in NW Greenland was "earlier than in the rest of Greenland." What is the evidence for later onset of warmth everywhere else? There is some evidence for early warmth in the east, including from Renland ice cap (which unlike most of the central Greenland ice core records and I think the very nice Buizert work, is elevation-corrected). Suggest just removing this statement that generalizes across all of Greenland, and keeping your discussion focused on the evidence for timing of warmth in the Nares Strait region vs a bit further south in NW Greenland, as you already mostly do.
Answer: We have deleted the statement as suggested.

Also, given the dearth of diverse evidence for atmospheric temperatures themselves in the Nares Strait region, it would be interesting to see a more fleshed-out discussion of the possible climate interpretations of the ice sheet history. Is it possible that the ice margin history is somehow compatible with early Holocene peak temperatures (more sensitive to ocean temperatures, longer lag in ice sheet equilibrium, more sensitive to precip??), or does the ice margin history truly preclude that?

Answer: We have added a part in section 5.4 about the possible effects from the Innuitian Ice Sheet on the western north GrIS during early Holocene. Following these lines, we already commented on the effects of rising temperatures and the opening of Nares Strait on the north GrIS margin and its retreat.

Figure 9: I don't think I've seen ice margin histories summarizes in quite this way visually before, and I really like it! Useful way to represent the data across a range of studies.

Answer: Thank you!

General point on the Discussion: One major conclusion of the cited Reusche study nearby is that the ice margin responded to cold events _9.3 or 8.2 ka, interrupting rapid retreat in the early Holocene. That should probably be acknowledged and discussed at least briefly. Do the new data generated in the current study add to or modify that picture?

Answer: In section 2, Study site and previous work, we briefly mention the study of Reusche et al and the possible stillstand of the ice sheet at 8.2 ka. Further, in section 5.2, we discuss the exposure ages from Humboldt Glacier in connection to the study from Reusche et al: Farthest north in Inglefield Land, at the southern flank of the Humboldt Glacier the ice margin reached its present-day extent already by c. 8.2 ka (Fig. 7a). This age is consistent with the ^{10}Be chronology from the northern flank of Humboldt Glacier where a moraine a few hundred meters outside the LIA moraine was abandoned c. 8.3 ka (Reusche et al., 2018). We have therefore not added anything further to the text about this.

Discussion, _line 310 etc: While invoking ocean temperatures to drive mid-Holocene minimum ice extent, it is also worth noting that many paleotemperature proxies from Greenland and Agassiz indicate that air temperatures were elevated above those of the late Holocene and even the 20th Century well into the middle Holocene. Could the minimum ice extent in the mid Holocene alternately represent a lagged equilibrium with warmer-than-20th C temperatures?

Answer: We believe that the rising sea surface temperatures in middle Holocene were the main driver of the smaller than present-day extent of the ice sheet in northwest Greenland. But it is likely that warming sea surface temperatures boosted a trend already happening from high atmospheric temperatures. We have added a few lines to section 5.4.

Interactive comment on “Glacial history of
Inglefield Land, north Greenland from combined
in-situ 10Be and 14C exposure dating” by Anne
Sofie Søndergaard et al.

Anonymous Referee #2
Received and published: 7 July 2020

The paper by Søndergaard et al. provides new CRN exposure ages (10Be, 14C) from erratic boulders and pebbles and radiocarbon ages from wood fragments to constrain the glacial history in Inglefield Land in northern Greenland. Based on their data, the authors conclude that that the glacial history in Inglefield Land commenced around 8.5 ka along the western margin and around 7.9 ka in the central part and reached is present position in the central part of the Inglefield by 6.9 ka. An overview of the Northern-Northwestern Greenland Ice Sheet history was also summarized as part of the work, including potential climate forcings.

Overall, this is a very nice study and will make a nice addition to the literature. Like thetwo other reviewers, I have similar questions regarding Figure 5 and how it was constructed and some more detailed questions about the some of the data (e.g. lithologies of boulders). Rather than repeat their questions, some of which I also had, I have provided my figure related questions and a few other comments that I hope the authors will address prior to publication. Otherwise this is a very nice, succinct paper that I was very pleased to read and really liked. Great work folks!

Answer: Thank you!

Figure 3: It would be useful if the authors included the uncertainties on the figure. Perhaps just including the average 10Be and 14C uncertainty in the legend would suffice. This is important to readers who may not encounter these types of data often need some baseline to who precise the measurements can be. Authors choice on this one since I’m only suggesting it.

Answer: We have added range and average of age uncertainties in the figure caption and refer readers to Table 1 if they want more specific information on individual samples.

Figure 4: I’m not sure I find this figure particularly useful. Does it provide anything more that the table doesn’t already provide the reader?

Answer: The figure does not provide more information than the table does, but we find it useful to represent data in a figure for better overview and clarity of the age distribution between the two glaciers and two sample materials.

Figure 5: I have the same sentiments as Nicolas on this, so will let you address his comment.

Answer: We have decided to change figure 5, so it now includes the original figure (a) as well as a model run (b) where we start the model at 60 ka, as describe in our response to Nicolas Young. We thought it would be good for the reader to have both scenarios in the main text, as it is an important point in the conclusion as to why the sample is affected by inheritance. We have changed the caption for figure 5 accordingly and also added a modified version of our response to Nicolas Young in the main text in section 5.1, where we describe why we have chosen the age constraints for our model the way we have.

Figure 7b: How does this work compare with the raised beach records from Bennike, 2002 or the modeling work from Lecavalier et al. 2017? The schematic in part b of this figure is interesting and makes me wonder how it might compare to those relative sea level curves and ice margin reconstructions. It might be worth mentioning something in this regard within the text.

Answer: The schematic part in Figure 7b is partly based on our results and partly on previous work (some of it used in Bennike (2002), which we mention in the discussions section 5.2. In this section we specifically discuss our result in relation to previous studies and how to find the best fit from both regarding the ice sheet history.

Figure 8b: I like these figures that the authors provide. However, it isn't clear to me how they derive some of these numbers. For instance, in Washington Land to the north of their site the authors provide an outer coastal retreat around 9.0 ka and present day ice margin around 8.6 ka. Based on my read of the Ceperley et al. 2020 paper, it seems like the ice margin was at Crozier Island at 8.5 ka and within the interior around 7.6 ka based on taking the youngest 10Be ages. These ages are consistent with what is being found in Inglefield Land and would indicate to me that over this entire area in the Northwest that the glaciers were largely acting in unison with no significant leads/lags. Perhaps the authors have recalculated these ages which is the reason for the discrepancy but regardless this should be addressed and explained assuming this is the case.

Answer: For the outer coast estimate at 9.0 ka, we have taken the mean which Ceperly et al. 2020 provide from Cozier Island and Joe Island. We find this mean representative for an outer coast deglaciation age of Washington Land: "The Holocene exposure ages from Crozier Island and Joe Island within Nares Strait have a mean of 9.0 ± 1.1 ka (n . 7; 1-s)."
For the inner coast estimate at 8.6 ka, we chose the average for "widespread ice sheet retreat" in Washington Land as stated by the authors. We acknowledge that a better estimate for when the ice what at its present-day extent might be the estimate from the authors at 6.9 ka for when "widespread glacial ice was absent". We have therefore changed the estimate for the inner coast deglaciation accordingly in the text (section 5.3) and Figure 8b.

Lines 209-210: I'm not sure how you get inheritance for 14C in this region but I agree with the authors that this age seems unrealistic. Based on Figure 5, the authors have suggested that during MIS 3 this location was ice free. This is a really interesting hypothesis and I think the authors should explain how this might be possible (e.g. climatically,glaciologically) given most people typically don't think of MIS 3 as that much different than the LGM, yet the authors Figure 5 would make MIS 3 seems similar to the present day. More should be said here since this hypothesis has some implications for what the climate might be like in the past and the authors could weigh in on it.

Answer: Following our conclusion of the ^{14}C age being affected by inheritance we comment on the possibility of a smaller than present day extent of the GrIS during MIS3, which fits with other studies from northern Greenland, which have concluded the same: "This scenario is to some degree consistent with other studies in northern Greenland that suggest a restricted GrIS during MIS 3 (Larsen et al., 2018; Søndergaard et al., 2019) and a late coalescence of the GrIS and Inuitian Ice Sheet around 22 cal. ka BP (England, 1999)". In the following lines we state that we can't make any firm conclusion due to the lack of data, which is why we have not elaborated more on the specific climatic conditions which would cause a MIS3 comparable to our present-day situation.

Editor Decision: Publish subject to minor revisions (review by editor) (23 Aug 2020) by Irina Rogozhina
Comments to the Author:
Dear authors,

I have now gone through your responses to the reviews and the short comment and in most cases I agree with your strategies for addressing the concerns raised by the reviewers. I therefore encourage you to address these comments as fully as possible following and expanding upon your proposed strategies.
Thank you. We have elaborated more on all comments and made changes accordingly in the manuscript.

In addition, I would like you to include the ensemble of model experiments (and their setup) that you are describing in your reply to the short comment (by Nicolas Young) in the form of supplementary materials.
We have decided to change figure 5, so it now includes the original figure (a) as well as a model run (b) where we start the model at 60 ka, as describe in our response to Nicolas Young. After your comment, we thought it would be good for the reader to have both scenarios in the main text, as it is an important point in the conclusion as to why the sample is affected by inheritance. We have changed the caption for figure 5 accordingly and also added a modified version of our response to Nicolas Young in the main text in section 5.1, where we describe why we have chosen the age constraints for our model the way we have.

I agree with the authors that Figure 4 is a useful visualization of the table contents and should therefore be retained.
The figure remains in the manuscript as it was.

The common line in the reviewers' comments is the need for a better integration between the results of this study and the interpretation of paleoclimate evidence related to the major drivers of the reconstructed ice sheet behavior. Hence, I would like to see a more detailed analysis and discussion of this in the revised manuscript.
We have added to the discussion in various sections addressing the climate-ice interactions that were questioned by the reviewers. Especially, section 5.4 has been expanded specifically in accordance to the reviewer comments. Specifically, we comment on the effect from the retreating Inuitian Ice Sheet on ice retreat in northern Greenland, which might have delayed this and further we have also added information on the effect from rising SSTs on the ice sheet that we see in northwest Greenland.

Good luck with the implementation of the reviews. I look forward to seeing the new version of the manuscript.

Kind regards,

Irina

Glacial history of Inglefield Land, north Greenland from combined in-situ ^{10}Be and ^{14}C exposure dating

Anne Sofie Søndergaard[1], Nicolaj Krog Larsen[1,2], Olivia Steinemann[3], Jesper Olsen[4], Svend Funder[2], David Lundbek Egholm[1], Kurt Henrik Kjær[2]

[1]Department of Geoscience, Aarhus University, Høegh Guldbergs Gade 2, 8000 Aarhus C, Denmark
[2]Globe Institute, University of Copenhagen, Øster Voldgade 5-7, 1350 Copenhagen K, Denmark
[3]Department of Physics, Institute for Particle Physics and Astrophysics, ETH Zürich, Otto-Stern-Weg 5, 8093 Zürich, Switzerland
[4]Department of Physics and Astronomy, Aarhus University, Ny Munkegade 120, 8000 Aarhus C, Denmark

Correspondence to: Anne Sofie Søndergaard (annesofie@geo.au.dk)

Deleted:

Abstract. Determining the sensitivity of the Greenland Ice Sheet (GrIS) to Holocene climate changes is a key prerequisite for understanding the future response of the ice sheet to global warming. In this study, we present new information on the Holocene glacial history of the GrIS in Inglefield Land, north Greenland. We use ^{10}Be and in-situ ^{14}C exposure dating to constrain the timing of deglaciation in the area and radiocarbon dating of reworked molluscs and wood fragments to constrain when the ice sheet retreated behind its present-day extent. The ^{10}Be ages are scattered ranging from c. 92.7 to 6.8 ka whereas the in-situ ^{14}C ages range from c. 14.2 to 6.7 ka. Almost half of the apparent ^{10}Be ages predate the Last Glacial Maximum and up to 89 % are to some degree affected by nuclide inheritance. Based on the few reliable ^{10}Be ages, the in-situ ^{14}C ages and existing radiocarbon ages from Inglefield Land, we find that the deglaciation along the coast commenced c. 8.6-8.3 cal. ka BP in the western part and c. 7.9 ka in the central part, following the opening of Nares Strait and arrival of warm waters. The ice margin reached its present-day position c. 8.2 ka at the Humboldt Glacier and c. 6.7 ka in the central part of Inglefield Land. Radiocarbon ages of reworked molluscs and wood fragments show that the ice margin was behind its present-day extent from c. 5.8 to 0.5 cal. ka BP. After 0.5 cal. ka BP, the ice advanced towards its Little Ice Age position. Our results emphasize that the slowly eroding and possibly cold-based ice in north Greenland makes it difficult to constrain the deglaciation history based on ^{10}Be ages alone unless it is paired with in-situ ^{14}C ages. Further, combining our findings with those of recently published studies reveals distinct differences between deglaciation patterns of northwest and north Greenland. Deglaciation of the land areas in northwest Greenland occurred earlier than in north Greenland and periods of restricted ice extent were longer, spanning Middle and Late Holocene. Overall, this highlights past ice sheet sensitivity to Holocene climate changes in an area where little information was available just a few years ago.

Deleted: Exposing

Deleted: m

Deleted: l

Deleted: wards

1 Introduction

Information about the glacial history of the Greenland Ice Sheet (GrIS) is important to constrain its sensitivity to past and ongoing climate changes (Lecavalier et al., 2017; Larsen et al., 2018). Since the 1990s, mass loss from the GrIS has accelerated, coinciding with atmospheric warming, and the ice sheet appears extremely sensitive to this warming, especially in north Greenland, where the ablation area has expanded with 46 % (Khan et al., 2015; Noël et al., 2019). As a result, the relative contribution to sea level rise from the north GrIS has increased significantly primarily through enhanced runoff as well as ice discharge via calving and melting at the Humboldt Glacier front (Mouginot et al., 2019; Noël et al., 2019).

With the introduction of cosmogenic nuclide exposure dating, previously glaciated areas of Greenland have been systematically targeted and >1000 ^{10}Be exposure ages have been published within the last two decades (Sinclair et al., 2016). In consequence, the late glacial and Holocene glaciation history is well constrained in most areas of Greenland (Bennike and Björck, 2002; Funder et al., 2011; Sinclair et al., 2016). However, there are still areas where the deglaciation chronology is constrained by minimum limiting radiocarbon ages of mainly marine molluscs along the coast and where inland exposure ages are unavailable (Bennike and Björck, 2002; Funder et al., 2011). This is particularly true for north Greenland including Inglefield Land where the current knowledge is primarily based on studies from late 1960s and 1970s (Nichols, 1969; Tedrow, 1970).

Despite that, ^{10}Be exposure dating has shown to be an efficient tool for constraining the deglaciation of the GrIS, but the use of this method is not without pitfalls. The method assumes that the measured ^{10}Be concentration was produced in one single post-glacial exposure period without surface erosion, but a number of studies have demonstrated that this assumption does not always hold. A particular challenge arises when subglacial bedrock erosion is too slow to remove ^{10}Be inventories produced during earlier exposure periods, such as the previous interglacial. In such case, the resulting age is typically referred to as an *apparent ^{10}Be exposure age* in acknowledgment of the fact that this age typically exceeds the true exposure age (Kelly et al., 2008; Corbett et al., 2015; Farnsworth et al., 2018; Larsen et al., 2018; Søndergaard et al., 2019; Ceperley et al., 2020; Skov et al., 2020). This problem of ^{10}Be nuclide inheritance emphasizes the need for new methods in order to thoroughly constrain the glacial history in parts of Greenland where the ice is cold-based and inefficient erosion leads to widespread nuclide inheritance.

Deleted: cold subglacial thermal regime in many places dictates

Deleted: and

Here we use a combination of ^{10}Be and in-situ ^{14}C exposure dating of boulders and pebbles to overcome the problem of nuclide inheritance and constrain the Holocene deglaciation history of the GrIS in Inglefield Land, north Greenland. In addition, we use radiocarbon dating of reworked marine molluscs and wood fragments to constrain the Holocene timing of restricted ice extent in the study area. Finally, we review and assess the glacial history in northwest and north Greenland with both local and regional climate records in order to expand our knowledge of the long-term sensitivity of the GrIS to climate changes.

2 Study site and previous work

Inglefield Land is situated in north Greenland, between 78.2-79.1° N and 65.8-72.8° W and is bound to the south and east by the GrIS, to the west by Smith Sound and to the north by Kane Basin and Humboldt Glacier (Fig. 1). Humboldt Glacier drains c. 5 % of the GrIS into Nares Strait and has a varied velocity profile due to diverse bed topography and drainage networks (Rignot and Kanagaratnam, 2006; Hill et al., 2017; Livingstone et al., 2017). In addition to the marine terminating Humboldt Glacier, the land-based Hiawatha Glacier is present in the eastern part of Inglefield Land. Together with the GrIS, this glacier overlie the newly discovered Hiawatha impact crater which makes the ice form a half circular structure, characterized by ice that flows faster than the rest of the ice margin terminating on land in Inglefield Land (Kjær et al., 2018).

The region is a high-Arctic desert, with low precipitation rates of c. 100-150 mm per year, falling mostly as snow (Blake et al., 1992; Dawes, 2004). The bedrock in the area is composed of Paleoproterozoic granite and gneiss, Late Proterozoic sedimentary and volcanic rocks and Lower Paleozoic sedimentary rocks and shelf carbonates with Quaternary deposits close to the present-day ice margin (Dawes, 2004; Kolb et al., 2016). The relief is gently declining from 600-700 m a.s.l. close to the present-day ice margin towards the coast where meltwater channels and rivers cut the up to c. 400 m high plateaus composed of sedimentary rocks (Dawes, 2004).

During the Last Glacial Maximum (LGM) the GrIS and Inuitian Ice Sheet coalesced in Nares Strait and the ice flowed north- and southward from a saddle in Kane Basin (England et al., 2006). The southward flowing ice formed the Smith Sound Ice Stream (England et al., 2006; Jennings et al., 2019) and it is believed to have extended to the 600 m depth contour in northern Baffin Bay (Funder et al., 2011). Radiocarbon ages reveal that deglaciation of Nares Strait initiated at the northern entrance c. 11 cal. ka BP and southern entrance c. 10 cal. ka BP (Bennike and Björck, 2002; Jennings et al., 2011). The final deglaciation and opening of the Nares Strait have been debated but recent off shore studies together with a few terrestrial studies place the collapse of the ice saddle in Kane Basin and opening of Nares Strait between c. 9-8 cal. ka BP (Georgiadis et al., 2018; Jennings et al., 2019; Dalton et al., 2020). Recently, Jakobsen et al. (2018) and Reusche et al. (2018) proposed overall glacial retreat of the GrIS in north Greenland during the Holocene, but with a possible stillstand of the ice sheet and its outlet glaciers as a response to the 8.2 cold events. These studies further suggested a restricted extent of the ice sheet in Middle and Late Holocene, until c. 0.3 ka where the ice reached its Little Ice Age (LIA) position.

Deleted: m

Deleted: l

The glacial history of Inglefield Land comprises the history of the Smith Sound Ice Stream along the coast, and the history of the GrIS in Inglefield Land, as described by Nichols (1969), Tedrow (1970) and Blake et al. (1992), with additional evidence from the neighbouring Humboldt Glacier and Washington Land to the east by Bennike (2002) and Reusche et al. (2018). The deglaciation of the interior parts of Inglefield Land is less well known but a set of distinct moraine systems between the present-day ice margin and the coast line (Nichols, 1969) suggest that the GrIS made several stops or readvances during the overall deglaciation of Inglefield Land. Our current knowledge about the timing of deglaciation in Inglefield Land comprises a number of minimum limiting radiocarbon ages of raised marine deposits from the coastal areas that range from c. 8.6 to 6.6 cal. ka BP (Nichols, 1969; Blake et al., 1992; Mason, 2010). The marine limit in Inglefield Land has been determined at several locations and decreases from c. 90 m in the southwestern part of Inglefield Land to c. 65 m in the northeastern part of Inglefield Land (Nichols, 1969; Funder and Hansen, 1996).

3 Methods

3.1 Cosmogenic nuclide exposure dating

Cosmogenic nuclide exposure dating is a widely used method to constrain the deglaciation history of former glaciated areas (Gosse and Phillips, 2001; Ivy-Ochs and Kober, 2008; Balco, 2020). One of the most common used nuclides is ^{10}Be as it forms in the abundant mineral quartz, and is fairly easy to extract and measure by accelerator mass spectrometry. However, due to its relatively slow decay and long half-life (1.4x10^{6} yr), problems can arise in areas characterized by slow-moving cold-based ice as small rates of erosion hinder complete removal of nuclides "inherited" from prior exposures and thus, yield apparent exposure ages exceeding the length pf the last ice-free period (Heyman et al., 2011). Nuclide inheritance is present in samples throughout Greenland, particularly at high elevations away from glacial troughs and fjords (Kelly et al., 2008; Corbett et al., 2013; Håkansson et al., 2016; Young et al., 2020) but it seems to be especially frequent in north Greenland where several studies have shown more widespread nuclide inheritance (Farnsworth et al., 2018; Larsen et al., 2018; Søndergaard et al., 2019; Ceperley et al., 2020; Larsen et al., in press).
Measurements of in-situ produced ^{14}C in boulders and bedrock can however circumvent the nuclide inheritance problem and help to obtain more reliable exposure ages (Hippe, 2017; Graham et al., 2019). Due to its shorter half-life (5730 yr), in-situ ^{14}C is sensitive to radioactive decay on Late Quaternary and Holocene timescales as the concentration build up from prior exposure will rapidly decrease, when a surface is shielded from cosmic rays (Lifton et al., 2001; Hippe, 2017). As such, it is an optimal tool to solve the most recent deglaciation history of the GrIS. However, in-situ ^{14}C is still not the preferred nuclide for exposure dating as the extraction process is demanding despite many improvements and developments within recent years (Lifton et al., 2015; Goehring et al., 2019; Lupker et al., 2019). Still more robust information on the deglaciation history can be achieved by using combined measurements of ^{10}Be and ^{14}C as shown by previous studies (Corbett et al., 2013; Hippe, 2017; Young et al., 2018; Graham et al., 2019).

Deleted: l

3.1.1 ^{10}Be exposure dating

^{10}Be exposure dating of boulders and pebbles was used to constrain the most recent glacial history of Inglefield Land. A total of 25 boulder samples were collected, all resting on bedrock except for sample GL1732-GL1735, which were on top of two moraines in the western part of Inglefield Land (Fig. 1c). The lithology of boulders sampled were all granite or gneiss, matching the lithology in and around Inglefield Land, but due to the placement on bedrock and moraines we assume the boulders to be transported some distance before deposition. In addition, two samples consisting of quartz pebbles (GL1715 and GL1716) were collected on an outwash plain in the northeastern part of Inglefield Land. Samples were collected using a rock saw, hammer and chisel to cut out the top few centimetres of quartz bearing stable boulders (Fig. 2). With a hand-held Garmin e-trex 30 GPS, we recorded the latitude, longitude and elevation of each sample. The orientation of the rock surface and shielding by the surrounding topography were measured using a compass and clinometer, respectively. Elevations of the sampled boulders were all between 65 m a.s.l. and 542 m a.s.l., and thus, were all at or above the local marine limit of the area (Nichols, 1969; Blake et al., 1992; Funder and Hansen, 1996). We measured sample thicknesses with a caliper before the samples were crushed and sieved. This information was used to calculate the average thickness of each sample. For boulder and pebble samples we used the 250-700 µm fraction to isolate quartz and extract beryllium.

All samples were processed in the Cosmogenic Nuclide Laboratory at Department of Geoscience, Aarhus University following methods adapted from (Corbett et al., 2016). The $^{10}Be/^{9}Be$ ratios were measured at the Aarhus AMS Centre and all samples were blank corrected. Nuclide concentrations were normalized to the Beryllium standard ICN-01-5-4, with a $^{10}Be/^{9}Be$ value of 2.851×10^{-12} (Nishiizumi et al., 2007). Apparent ^{10}Be exposure ages were calculated using the online exposure age calculator formerly known as the CRONUS-Earth online exposure calculator v.3 (Balco et al., 2008) in combination with the Baffin Bay production rate (Young et al., 2013) and the Lm production scaling scheme (Lal, 1991; Stone, 2000). The rock density was set to 2.65 g/m^3 as it is representative for the boulders we sampled, and we assumed zero erosion. We did not correct for cover by vegetation or snow as the vegetation in the area is sparse and precipitation rates are low, c. 100-150 mm per year (Dawes, 2004). The sampled boulders were furthermore all positioned in open locations in the landscape making it highly unlikely that any snow cover persisted for long periods of time. As the glaciostatic uplift history is not well constrained in north Greenland, we present our ^{10}Be ages without any uplift correction, similarly to many other studies in Greenland which have shown the corrections to be negligible (Young et al., 2012; Sinclair et al., 2016; Larsen et al., 2018; Young et al., 2020).

All resulting apparent exposure ages and parameters used in the calculations can be seen in Table 1. The ^{10}Be ages are presented with 1σ analytical uncertainty and ages calculated using other scaling schemes deviate by <2 %.

3.1.2 In-situ ^{14}C exposure dating

We used in-situ ^{14}C exposure dating to further constrain the deglaciation history of Inglefield Land, primarily by testing for ^{10}Be nuclide inheritance in selected samples. Four of the quartz samples used for ^{10}Be exposure dating were chosen for in-situ ^{14}C exposure dating, GL1725, GL1712, GL1701 and GL1708. We chose these samples based on i) the resulting apparent ^{10}Be exposure ages within each sample location, ii) the amount of quartz left, and iii) the sample location in the study area to secure a broad spatial distribution (Fig. 1c). Approximately 4 g of purified quartz, the same used for ^{10}Be extraction, was used to extract the in-situ produced ^{14}C. Samples for in-situ ^{14}C measurements were processed using the in-situ ^{14}C extraction line at ETH Zürich (Hippe et al., 2009; Lupker et al., 2019). Samples were measured at ETH Zürich with the MICASAS AMS system (Synal et al., 2007; Wacker et al., 2010) and sample in-situ ^{14}C concentrations were calculated from measured $^{14}C/^{12}C$ ratios (Hippe and Lifton, 2016). In-situ ^{14}C ages were calculated using the online exposure age calculator formerly known as the CRONUS-Earth online exposure calculator v.3 (Balco et al., 2008), the west Greenland production rate (Young et al., 2014), and the Lm production scaling scheme (Lal, 1991; Stone, 2000). All resulting ages and variables used in the calculations are listed in Table 2. In-situ ^{14}C exposure ages are presented with 1σ analytical uncertainty and ages calculated using other scaling schemes deviate by <4 %.

3.2 Radiocarbon dating of reworked molluscs and wood fragments

Radiocarbon dating of reworked organic material in glacial deposits can be used to determine when the ice extent was smaller than present (Bennike and Weidick, 2001; Briner et al., 2014; Farnsworth et al., 2018). For this purpose, we therefore collected reworked marine molluscs from the surface of and within diamictic sediments at the southern margin of the Humboldt Glacier (Fig. 1c). From the samples site, 15 molluscs were chosen, pre-treated following the procedure of (Brock et al., 2010), and radiocarbon dated at the Aarhus AMS Centre (Olsen et al., 2016). In addition, four wood fragments were retrieved at 193 m a.s.l. on the meltwater plain next to the meltwater outlet at the Hiawatha Glacier (Fig. 1c). Due to the placement of the wood fragments at the tip of the glacier, we assume the wood to have been transported from underneath the glacier a distance up ice, before deposition at the glacier front. The wood fragments were collected together with sediment samples analysed in recent studies concerning the Hiawatha impact crater (Kjær et al., 2018; Garde et al., 2020). It was not possible to identify the dated wood fragments to species level. The four samples were pre-treated and radiocarbon dated at Beta Analytic.

Deleted: in front of

Deleted: The wood fragments were

Radiocarbon ages for the molluscs were calibrated using OxCal v4.3 (Ramsey, 2009) with the Marine13 calibration curve (Reimer et al., 2013) and a marine reservoir effect of 550 ^{14}C years (ΔR=150 ^{14}C a) based on a couple of ages from molluscs collected alive before 1960 in north Greenland (Mörner and Funder, 1990). Radiocarbon ages for the wood fragments were calibrated with the IntCal13 calibration curve (Reimer et al., 2013). Sample information, resulting radiocarbon ages, and calibrated ages are reported in Table 3. Throughout the text, we use the mean calibrated radiocarbon age ±2σ.

4 Results

4.1 ^{10}Be and in-situ ^{14}C exposure dating

^{10}Be exposure dating was carried out on 25 boulder samples and 2 samples consisting of pebbles to constrain the deglaciation of Inglefield Land (Fig. 3). The measured ^{10}Be concentrations in the 27 samples range from $3.0±0.9x10^4$ to $60.3±0.9x10^4$ ^{10}Be at/g and result in apparent exposure ages ranging from 92.7±1.5 ka to 6.8±2.0 ka, with the oldest ages being from boulders on moraines in the western part of the area and the younger ages resulting from boulders closer to Humboldt Glacier and the coast in the northeastern part of the area (Fig. 3, Table 1).

Although the ^{10}Be ages are scattered we see some structure in the dataset. There is no clear pattern between the lithology of the individual boulders sampled and the resulting exposure ages, but the majority of ages sampled below 300 m a.s.l. group within the post-LGM period, with a peak in Early Holocene whereas most samples above 450 m a.s.l. predate the LGM.

Deleted: e

Further, there also seem to be a vague pattern in spatial distribution, with the oldest ^{10}Be ages being from the two moraine ridges in western Inglefield Land and the youngest boulder ages closer to Humboldt Glacier.

In-situ ^{14}C exposure dating were carried out to better constrain the deglaciation of Inglefield Land from the scattered ^{10}Be ages. The measured in-situ ^{14}C concentrations in the four samples range from 8.4±0.3x10^4 to 17.4±0.2x10^4 at/g and resulted in exposure ages ranging from 14.2±0.5 ka to 6.7±0.3 ka (Fig. 3, Table 2). All in-situ ^{14}C ages are younger than the ^{10}Be ages resulting from the same quartz sample, confirming that the ^{10}Be ages are generally affected by nuclide inheritance. However, the in-situ ^{14}C ages do to some degree match the youngest ^{10}Be ages from the same localities, except for GL1701, which predate the Holocene. The remaining three in-situ ^{14}C ages group in Middle Holocene.

Deleted: m

4.2 Radiocarbon dating of reworked molluscs and wood fragments

Reworked marine molluscs were collected along the southern margin of the Humboldt Glacier (Fig. 1c). Several species were identified and 15 samples of *Mya truncata*, *Hiatella arctica* and *Astarte borealis* were used for radiocarbon dating. The calibrated mean radiocarbon ages range from 3.6±0.04 to 0.5±0.03 cal. ka BP (Fig. 4, Table 3) and reflect the period when the Humboldt Glacier was behind its present-day extent. In addition, the wood samples collected on the outwash plain in front of the Hiawatha Glacier resulted in ages between 5.8±0.06 cal. ka BP and 1.9±0.04 cal. ka BP (Fig. 4, Table 3). As the wood fragments were retrieved right in front of the Hiawatha Glacier, the wood fragments are more likely to have originated from underneath the glacier than being transported from a nearby soil to the sample site by wind or water. We therefore believe these ages to constrain a time when the glacier was smaller than its present-day extent.

Deleted: from the surface of and within diamictic sediments

Deleted: western

5 Discussion

5.1 Indications of low erosion rates and cold-based ice in north Greenland

The ^{10}Be ages from Inglefield Land are scattered which makes it difficult to fully constrain the glacial history in the area. We consider the 12 ^{10}Be ages older than the LGM as evidence of nuclide inheritance from prior exposure (Fig. 3) and discard them as constraints of the glacial history in Inglefield Land. Of the remaining 15 samples postdating the LGM, some do most likely also reflect nuclide inheritance. Within uncertainty, only four of the 15 post-LGM ^{10}Be ages overlap with the three youngest in-situ ^{14}C ages. Thus, by including in-situ ^{14}C ages in the analysis we determine that 11 of the post-LGM ^{10}Be ages are affected by inheritance and thus, overestimate the post-LGM exposure period to a varying degree. In total, 24 out of 27 samples (c. 89 %) from Inglefield Land show some degree of nuclide inheritance.

We also consider the oldest in-situ ^{14}C age of c. 14.2 ka to be affected by inheritance as it is unlikely that Inglefield Land was deglaciated at that time. Different modelled scenario of nuclide build up that almost reach the measured concentration of the sample and still follow the known glacial history of the GrIS in north Greenland is seen in Figure 5. In scenario the first

Deleted: The only

sscenario. Inglefield Land was deglaciated during MIS 3 from 45 to 23 ka and again in Holocene from 6.7 ka until present. This limits the expansion of the GrIS during the LGM to a narrow interval from c. 23 to 7 ka. This scenario is to some degree consistent with other studies in northern Greenland where radiocarbon ages of marine molluscs show that the GrIS in the study areas had a restricted ice extent during MIS 3, starting as early as c. 42 cal. ka BP (Larsen et al., 2018; Søndergaard et al., 2019) and a late coalescence of the GrIS and Inuitian Ice Sheet around 22 cal. ka BP (England, 1999). We have tried different model runs, including letting the initial concentration being at saturation (starting the model at 60 ka), but due to the short half-life of ^{14}C, any concentration build-up prior to our constrained period only result in a very small increase in the final present-day concentration (c. 5%). It is therefore not exposure prior to 45 ka, that is the main reason for the remaining "inheritance". However, as we only have one datapoint and the simulation is incapable of fully reaching the measured concentration we cannot make any firm conclusions on the timing of prior exposure of the sample and the implications for the ice sheet history. The trend between apparent ^{10}Be ages and elevation of the samples points towards larger amount of inheritance in samples from higher elevations (Fig. 6). This pattern has also recently been observed in adjacent Washington Land as well as in Dove Bugt, northeast Greenland (Ceperley et al., 2020; Skov et al., 2020). In addition, there is an increasing amount of inheritance in samples farther away from the Humboldt Glacier. This spatial distribution of samples with inheritance at higher elevations away from the Humboldt Glacier is expected as these locations represent areas outside troughs where erosion is low because of slowly moving or even cold-based ice. A similar relationship between nuclide inheritance and elevation and distance to deep fjords with large fast flowing outlet glaciers indicative of higher erosion rates has been demonstrated elsewhere in Greenland (Larsen et al., 2014; Søndergaard et al., 2019).

Overall, inheritance and the lack of sufficient nuclide resetting is a widespread problem especially in north Greenland, and have complicated several studies within recent years (Corbett et al., 2015; Farnsworth et al., 2018; Søndergaard et al., 2019; Ceperley et al., 2020; Larsen et al., in press). Thus, we conclude that large parts of the north GrIS were inefficient at eroding the subglacial topography during parts of or throughout the last glaciation probably because subglacial sliding were limited by cold-based thermal conditions and the overall low ice flux resulting from the relatively small precipitation rates of the region. We note that cold-based zones are also considered to dominate the present-day thermal state of the GrIS (MacGregor et al., 2016).

5.2 Holocene glacial history of Inglefield Land

During the LGM, Inglefield Land was completely ice covered and the ice nourished the Smith Sound Ice Stream primarily through the Humboldt Glacier until the opening of Nares Strait sometime between c. 9 and 8 cal. ka BP (Georgiadis et al., 2018; Jennings et al., 2019; Dalton et al., 2020). The outer coast at Kap Inglefield Land, Kap Grinell and Renselaer Bay in southwest Inglefield Land was deglaciated between c. 8.6 and 8.3 cal. ka BP (Nichols, 1969; Blake et al., 1992; Mason, 2010). Farther north, the deglaciation of the outer coast at Marshall Bay in central Inglefield Land is constrained to c. 7.9 ka by a

Deleted: this scenario

Deleted:

Deleted: that suggest a restricted GrIS single in-situ ^{14}C age. This age is largely consistent with a radiocarbon age of marine molluscs of c. 8.2 cal. ka BP at Minturn Elv located c. 20 km east of Marshall Bay (Nichols, 1969) (Fig. 7a).

After reaching the outer coast, the ice margin continued its retreat towards its present-day position which was reached by c. 6.7 ka in the central part of Inglefield Land. Farther north, the ice probably retreated somewhat slower as suggested by dating of a rearrangement of the meltwater drainage pattern from the Hiawatha Glacier. Initially, meltwater flowed from the Hiawatha Glacier towards Dallas Bay, but this changed when the ice margin was approximately halfway between the coast and present-day extent where a water divide then rerouted the meltwater towards Marshall Bay (Nichols, 1969). The timing of this change is constrained by a single ^{10}Be age of meltwater deposits (pebble sample) that yield an age of c. 6.8 ka (Fig. 7b). The ^{10}Be age is, however, consistent with a radiocarbon age of molluscs, presumably from lower lying prodeltaic sediments, which gave an age of c. 6.6 cal. ka BP at Dallas Bay (Nichols, 1969). This suggests that the ice margin was located north of the meltwater drainage divide around c. 6.8 ka. Farthest north in Inglefield Land, at the southern flank of the Humboldt Glacier the ice margin reached its present-day extent already by c. 8.2 ka (Fig. 7a). This age is consistent with the ^{10}Be chronology from the northern flank of Humboldt Glacier where a moraine a few hundred meters outside the LIA moraine was abandoned c. 8.3 ka (Reusche et al., 2018).

After the ice margin reached its present-day position it continued to retreat farther inland. Wood fragments in front of the Hiawatha Glacier demonstrate that the land-based part of the GrIS in Inglefield Land was smaller than present between c. 5.8 and 1.9 cal. ka BP. In addition, the age distribution of the molluscs collected at the Humboldt Glacier margin indicates that it was behind its present-day position between c. 3.6 to 0.5 cal. ka BP (Fig. 7a). At the northern flank of Humboldt Glacier, radiocarbon ages of reworked marine molluscs suggest that the glacier retreated at least 25 km farther inland between c. 3.7 and 0.3 cal. ka BP (Bennike, 2002) possibly favoured by the bed topography being below sea level 10's of km inland (Morlighem et al., 2014; Morlighem et al., 2017). Thus, no later than c. 0.3 cal. ka BP, the GrIS in Inglefield Land re-advanced towards its LIA maximum extent. The spatial extent of the Late Holocene retreat of the Hiawatha Glacier behind its present-day ice margin is not known, but the ice retreat may possibly have exposed parts of the Hiawatha impact crater (Fig. 7b).

Deleted: l

5.3 A review of the Holocene glacial history in northwest and north Greenland

In the following we review the new data from north and northwest Greenland to put our results into a broader context. We focus on two stages of the deglaciation history of the GrIS, namely when it i) deglaciated from the coast towards its present-day extent and ii) when it was smaller than present (Fig. 8). For information about the offshore deglaciation history, the reader is referred to recent reviews by Georgiadis et al. (2018), Jennings et al. (2019) and Dalton et al. (2020).

In the southern part of northwest Greenland, the ice margin reached the outer coast near Upernavik c. 11.3 ka (Corbett et al., 2013) coinciding with the overall ice retreat in Melville Bay initiating c. 11.6 ka (Søndergaard et al., 2020) (Fig. 8b). The ice reached the inner part of Upernavik Fjord c. 9.9 ka (Briner et al., 2013) and in Melville Bay the ice was at its present-day extent already c. 11.5 ka (Søndergaard et al., 2020) (Fig. 8b). Farther north, coastal deglaciation near Thule and Delta Sø began

Deleted: (Søndergaard et al., in review)

Deleted: (Søndergaard et al., in review)

c. 10.8 ka (Corbett et al., 2015; Axford et al., 2019) and the ice margin reached its present-day extent at nearby Wax Lips Lake c. 10.1 ka (McFarlin et al., 2018). In Inglefield Bredning north of Thule the ice reached the inner parts of the fjord c. 11.9 ka (Søndergaard et al., 2019) (Fig. 8b). In north Greenland, results from Inglefield Land show that the deglaciation of the outer coast commenced c. 8.6 cal. ka BP in southeast and c. 7.9 ka in the central part of the coast line and the ice reached its present-day position in central Inglefield Land c. 6.7 ka. The Humboldt Glacier deglaciated and reached its present-day extent c. 8.2 ka. In the adjacent Washington Land, deglaciation of the outer coast is constrained to c. 9.0 ka with widespread deglaciation of the entire area evident c. 8.6 ka and absence of widespread glacial ice no later than 6.9 ka (Ceperley et al., 2020). Farther north, Petermann Glacier was positioned at the outer sill in Hall Basin c. 8.7 (Jakobsson et al., 2018) and it reached its present day position c. 6.9 ka (Reilly et al., 2019).

Restricted ice extent behind the present-day ice margin in northwest and north Greenland was widespread during large parts of Middle and Late Holocene. In Upernavik and Melville Bay, the ice sheet was behind its present-day position between c. 9.1 and 0.4 cal. ka BP (Bennike, 2008; Briner et al., 2013; Briner et al., 2014; Axford et al., 2019; Søndergaard et al., 2020) (Fig. 8c). Farther north, mosses from a local ice cap and subfossil plants from the GrIS show a smaller than present-day extent before c. 3.3 cal. ka BP around Qaanaaq and throughout most of the Holocene until c. 1850 AD in the Thule area (Farnsworth et al., 2018; Axford et al., 2019; Søndergaard et al., 2019). In Inglefield Land, north Greenland, wood fragments in front of the Hiawatha Glacier suggest that the ice margin was behind its present-day extent from c. 5.8 and 1.9 cal. ka BP, whereas the Humboldt Glacier retreated at least 25 km inland c. 3.7 to 0.3 cal. ka BP (Bennike, 2002). The Petermann Glacier farther north also retreated farther inland of its present-day position and following readvance reached its LIA extent c. 0.3 ka (Reusche et al., 2018; Reilly et al., 2019) (Fig. 8c).

In summary, the timing of deglaciation along the coast in northwest Greenland is earlier than in north Greenland around Nares Strait, but the timing is, however, in accordance with the overall deglaciation in Greenland (Bennike and Björck, 2002; Funder et al., 2011). Further, the periods of Middle and Late Holocene restricted ice extent of the larger outlet glaciers in north Greenland initiated later than in northwest Greenland and was shorter.

5.4 Holocene ice and climate interactions in northwest and north Greenland

The contrasting pattern of deglaciation between northwest and north Greenland, can in part be explained by different responses of the two sectors to Holocene climate changes (Fig. 9). The early deglaciation of the land areas in northwest Greenland from Upernavik to Inglefield Bredning coincides with the Early Holocene Thermal Maximum (HTM) (c. 11-8 ka) in northwest Greenland (Lecavalier et al., 2017; Axford et al., 2019) (Fig. 9a-c). This rapid increase in surface air temperatures has been suggested to be the main driver of the widespread rapid deglaciation specifically in Melville Bay, the Thule area and Inglefield Bredning (Axford et al., 2019; Søndergaard et al., 2019; Søndergaard et al., 2020), showing the sensitivity of marine based ice to rising air temperatures.

Deleted: Delta Sø

Deleted:

Deleted: (Axford et al., 2019)

Deleted: m

Deleted: l

Deleted: Farther north in the Thule area and around Qaanaaq, mosses from a local ice cap and subfossil plants from the GrIS show a smaller ice extent before c. 3.3 cal. ka BP

Deleted: m

Deleted: l

Deleted: e

Deleted: which initiated earlier than in the rest of Greenland (Briner et al., 2016; Buizert et al., 2018)

Despite elevated temperatures being above those of the Late Holocene in north Greenland during Early Holocene and parts of Middle Holocene, it is possible that the effects of the retreating Innuitian Ice Sheet, which still covered Ellesmere Island during Early Holocene, to some degree dampened the effect from the high atmospheric temperatures on the GrIS and its outlets in western north Greenland during this period (Briner et al., 2016; Dalton et al., 2020). Further it has been suggested that warm Atlantic waters in Hall Basin, northern Nares Strait, assisted Early Holocene ice retreat (Jennings et al., 2011), warm waters and increasing ocean temperatures in southern Nares Strait seemed to arrive later than along the west Greenland coast (Dyke et al., 1996; Levac et al., 2001; Lecavalier et al., 2017; Axford et al., 2019). This delay in warming ocean conditions in southern Nares Strait might be the reason why the opening of Nares Strait and the deglaciation of the coastal areas in Inglefield Land and Washington Land happened 2-3 ka later than the land areas in northwest Greenland (Bennike and Björck, 2002; Larsen et al., 2014; Sinclair et al., 2016; Larsen et al., 2019).

Deleted: Although

Deleted: e

After the ice margin reached its present-day extent in north and northwest Greenland it continued to retreat farther inland. In northwest Greenland, the period with restricted ice extent in Melville Bay c. 9.1 to 0.4 cal. ka BP, was driven by a strengthening of the West Greenland Current and warm ocean waters arriving in Middle Holocene (Levac et al., 2001; Caron et al., 2020) (Fig. 9d). The presence of *Chlamys islandica* infers that the period with marine based outlets were behind their present-day extent in North Greenland coincides with the arrival of warm waters in Nares Strait (Bennike, 2002). Warming sea surface temperatures drove Middle Holocene ice sheet retreat especially in northwest Greenland, but the overall retreat possibly was initiated by and still affected from Early Holocene rising atmospheric temperatures.

Deleted: m

The Neoglacial cooling are known to have affected ice on land in northwest Greenland and resulting in expansion of local ice caps, lake ice cover and even parts of the northwest GrIS (Blake et al., 1992; Lasher et al., 2017; Farnsworth et al., 2018; Søndergaard et al., 2019). The Hiawatha Glacier in north Greenland show a re-advance after c. 1.9 cal. ka BP, as a possible response to the Neoglacial cooling, which also seems to have provoked a readvance of the Petermann Glacier c. 2.8 ka (Reusche et al., 2018). Finally, the ice in north and northwest Greenland show a near synchronous re-advance towards its LIA extents which coincides with the LIA cooling within the last millennium (Lasher et al., 2017; Lecavalier et al., 2017; Axford et al., 2019).

6 Conclusion

In this study we used in-situ ^{10}Be and ^{14}C cosmogenic nuclide exposure dating and radiocarbon dating of reworked organic material to constrain the Holocene glacial history of Inglefield Land, north Greenland. Our results revealed a large scatter in the ^{10}Be ages with c. 45 % of the ages predating the LGM and an overall 89 % of the samples being affected by inheritance possibly due to low-erosive cold-based ice. We find that the outer coast in Inglefield Land began to deglaciate between c. 8.6 and 8.3 cal. ka BP in the southeastern part, whereas the central part was deglaciated by c. 7.9 ka. Following initial deglaciation, the ice margin reached its present-day position c. 6.7 ka in central Inglefield Land, whereas Humboldt Glacier in the northern part of the study area reached its present extent already by c. 8.2 ka. After deglaciation the ice margin retreated behind its present-day extent from c. 5.8 to 1.9 cal. ka BP at the Hiawatha Glacier and c. 3.7 to 0.3 cal. ka BP at the Humboldt Glacier. Thus, the readvance towards the LIA extent initiated between 1.9 and 0.3 cal. ka BP.

We furthermore reviewed new data from north and northwest Greenland to put our results into a broader context and assessed the findings with local and regional climate records. We find that the Holocene glacial history varies significantly between northwest and north Greenland. The deglaciation from the coast to the present-day ice extent in northwest Greenland occurred at the onset of the Holocene, possibly as a response to the relatively early HTM. Deglaciation continued and the ice sheet retreated behind its present-day extent in northwest Greenland throughout most of Middle and Late Holocene driven by continued high air temperatures and the arrival of warm waters along the west Greenland coast. Contrary, the deglaciation of the outer coast in Nares Strait and north Greenland was delayed c. 2-3 ka and show a more restricted period of retreat behind its present-day extent. The observed difference in pattern of deglaciation in the two regions is most likely a consequence of the large marine based part of the northwest GrIS being more sensitive to climate changes as opposed to the largely land based north GrIS. Further, the late opening of Nares Strait could have delayed ice retreat in north Greenland, despite early atmospheric warming. During the LIA cooling, the GrIS do though show a synchronous response with ice advance throughout north and northwest Greenland. Our findings highlight the complexity of the ice-climate system and show clear differences in ice sheet sensitivity between northwest and north Greenland. As such, this add new knowledge and possible constraints on the future state of the GrIS as a response to present-day global warming.

Deleted: m

Deleted: l

Author contribution

N.K.L, K.H.K, S.F and A.S.S participated in fieldwork and decided on the sampling strategy. A.S.S did ^{10}Be sample preparation and J.O. and A.S.S carried out measurements and calculation. O.S and A.S.S carried out in-situ ^{14}C sample preparation, measurements and calculation. A.S.S and N.K.L made initial interpretations of the results and wrote the paper with contribution from the co-authors.

Acknowledgement

This research was supported by Aarhus University Research Foundation and the Villum Foundation. Birte Lindahl Eriksen and Rikke Brok Jensen are thanked for extensive help in the laboratory. We also thank the Carlsberg Foundation for supporting this study.

References

Axford, Y.,Lasher, G. E.,Kelly, M. A.,Osterberg, E. C.,Landis, J.,Schellinger, G. C.,Pfeiffer, A.,Thompson, E. & Francis, D. R. 2019. Holocene temperature history of northwest Greenland – With new ice cap constraints and chironomid assemblages from Deltasø. *Quaternary Science Reviews,* 215**,** 160-172.

Balco, G. 2020. Glacier Change and Paleoclimate Applications of Cosmogenic-Nuclide Exposure Dating. *Annual Review of Earth and Planetary Sciences,* 48**,** 1.1-1.28.

Balco, G.,Stone, J. O.,Lifton, N. A. & Dunai, T. J. 2008. A complete and easily accessible means of calculating surface exposure ages or erosion rates from 10Be and 26Al measurements. *Quaternary Geochronology,* 3**,** 174-195.

Bennike, O. 2002. Late Quaternary history of Washington Land, North Greenland. *Boreas,* 31**,** 260-272.

Bennike, O. 2008. An early Holocene Greenland whale from Melville Bugt, Greenland. *Quaternary Research,* 69**,** 72-76.

Bennike, O. & Björck, S. 2002. Chronology of the last recession of the Greenland Ice Sheet. *Journal of Quaternary Science,* 17**,** 211-219.

Bennike, O. & Weidick, A. 2001. Late Quaternary history around Nioghalvfjerdsfjorden and Jøkelbugten, North-East Greenland. *Boreas,* 30**,** 205-227.

Formatted: Danish

Blake, W.,Boucherle, M. M.,Fredskild, B.,Janssens, J. A. & Smol, J. P. 1992. The geomorphological setting, glacial history and Holocene developement of "Kap Inglefield Sø", Inglefield Land, North-West Greenland. *Meddelelser om Grønland, Geoscience,* 27.

Formatted: Danish

Briner, J. P.,Håkansson, L. & Bennike, O. 2013. The deglaciation and neoglaciation of Upernavik Isstrøm, Greenland. *Quaternary Research,* 80**,** 459-467.

Briner, J. P.,Kaufman, D. S.,Bennike, O. & Kosnik, M. A. 2014. Amino acid ratios in reworked marine bivalve shells constrain Greenland Ice Sheet history during the Holocene. *Geology,* 42**,** 75-78.

Briner, J. P.,Mckay, N. P.,Axford, Y.,Bennike, O.,Bradley, R. S.,De Vernal, A.,Fisher, D.,Francus, P.,Fréchette, B.,Gajewski, K.,Jennings, A.,Kaufman, D. S.,Miller, G.,Rouston, C. & Wagner, B. 2016. Holocene climate change in Arctic Canada and Greenland. *Quaternary Science Reviews,* 147**,** 340-364.

Brock, F.,Higham, T.,Ditchfield, P. & Ramsey, C. B. 2010. Current Pretreatment Methods for AMS Radiocarbon Dating at the Oxford Radiocarbon Accelerator Unit (Orau). *Radiocarbon,* 52**,** 103-112.

Buizert, C.,Keisling, B. A.,Box, J. E.,He, F.,Carlson, A. E.,Sinclair, G. & Deconto, R. M. 2018. Greenland-Wide Seasonal Temperatures During the Last Deglaciation. *Geophysical Research Letters,* 45**,** 1905-1914.

Caron, M.,Montero-Serrano, J. C.,St-Onge, G. & Rochon, A. 2020. Quantifying provenance and transport pathways of Holocene sediments from the northwestern Greenland margin. *Paleoceanography and Paleoclimatology*.

Ceperley, E. G.,Marcott, S. A.,Reusche, M. M.,Barth, A. M.,Mix, A. C.,Brook, E. J. & Caffee, M. 2020. Widespread early Holocene deglaciation, Washington Land, northwest Greenland. *Quaternary Science Reviews,* 231.

Corbett, L. B.,Bierman, P. R.,Graly, J. A.,Neumann, T. A. & Rood, D. H. 2013. Constraining landscape history and glacial erosivity using paired cosmogenic nuclides in Upernavik, northwest Greenland. *Geological Society of America Bulletin,* 125**,** 1539-1553.

Corbett, L. B.,Bierman, P. R.,Lasher, G. E. & Rood, D. H. 2015. Landscape chronology and glacial history in Thule, northwest Greenland. *Quaternary Science Reviews,* 109**,** 57-67.

Corbett, L. B.,Bierman, P. R. & Rood, D. H. 2016. An approach for optimizing in situ cosmogenic 10 Be sample preparation. *Quaternary Geochronology,* 33**,** 24-34.

Dalton, A. S.,Margold, M.,Stokes, C. R.,Tarasov, L.,Dyke, A. S.,Adams, R. S.,Allard, S.,Arends, H. E.,Atkinson, N.,Attig, J. W.,Barnett, P. J.,Barnett, R. L.,Batterson, M.,Bernatchez, P.,Borns, H. W.,Breckenridge, A.,Briner, J. P.,Brouard, E.,Campbell, J. E.,Carlson, A. E.,Clague, J. J.,Curry, B. B.,Daigneault, R.-A.,Dubé-Loubert, H.,Easterbrook, D. J.,Franzi, D. A.,Friedrich, H. G.,Funder, S.,Gauthier, M. S.,Gowan, A. S.,Harris, K. L.,Hétu, B.,Hooyer, T. S.,Jennings, C. E.,Johnson, M. D.,Kehew, A. E.,Kelley, S. E.,Kerr, D.,King, E. L.,Kjeldsen, K. K.,Knaeble, A. R.,Lajeunesse, P.,Lakeman, T. R.,Lamothe, M.,Larson, P.,Lavoie, M.,Loope, H. M.,Lowell, T. V.,Lusardi, B. A.,Manz, L.,Mcmartin, I.,Nixon, F. C.,Occhietti, S.,Parkhill, M. A.,Piper, D. J. W.,Pronk, A. G.,Richard, P. J. H.,Ridge, J. C.,Ross, M.,Roy, M.,Seaman, A.,Shaw, J.,Stea, R. R.,Teller, J. T.,Thompson, W. B.,Thorleifson, L. H.,Utting, D. J.,Veillette, J. J.,Ward, B. C.,Weddle, T. K. & Wright, H. E. 2020. An updated radiocarbon-based ice margin chronology for the last deglaciation of the North American Ice Sheet Complex. *Quaternary Science Reviews,* 234.

Dawes, P. R. 2004. Explanatory notes to the Geological map of Greenland, 1:500 500, Humbolt Gletscher, Sheet 6. *Geological Survey of Denmark and Greenland Map Series* 1**,** 1-48.

Dyke, A. S.,Dale, J. E. & Mcneely, R. N. 1996. Marine Molluscs as Indicators of Environmental Change in Glaciated North America and Greenland During the Last 18 000 Years. *Géographie physique et Quaternaire,* 50.

England, J. 1999. Coalescent Greenland and Innuitian ice during the Last Glacial Maximum: revising the Quaternary of the Canadian High Arctic. *Quaternary Science Reviews,* 18**,** 421-46.

England, J.,Atkinson, N.,Bednarski, J.,Dyke, A. S.,Hodgson, D. A. & Ó Cofaigh, C. 2006. The Innuitian Ice Sheet: configuration, dynamics and chronology. *Quaternary Science Reviews,* 25**,** 689-703.

Farnsworth, L. B.,Kelly, M. A.,Bromley, G. R. M.,Axford, Y.,Osterberg, E. C.,Howley, J. A.,Jackson, M. S. & Zimmerman, S. R. 2018. Holocene history of the Greenland Ice-Sheet margin in Northern Nunatarssuaq, Northwest Greenland. *arktos,* 4.

Funder, S. & Hansen, L. 1996. The Greenland ice sheet - a model for its culmination and decay during and after the last glacial maximum. *42*.

Funder, S.,Kjeldsen, K. K.,Kjær, K. H. & Ó Cofaigh, C. 2011. The Greenland Ice Sheet During the Past 300,000 Years: A Review. 15, 699-713.

Garde, A. A.,Søndergaard, A. S.,Guvad, C.,Dahl-Møller, J.,Nehrke, G.,Sanei, H.,Weikusat, C.,Funder, S.,Kjær, K. H. & Larsen, N. K. 2020. Pleistocene organic matter modified by the Hiawatha impact, northwest Greenland. *Geology*.

Georgiadis, E.,Giraudeau, J.,Martinez, P.,Lajeunesse, P.,St-Onge, G.,Schmidt, S. & Massé, G. 2018. Deglacial to postglacial history of Nares Strait, Northwest Greenland: a marine perspective. *Climate of the Past Discussions***,** 1-29.

Goehring, B. M.,Wilson, J. & Nichols, K. 2019. A fully automated system for the extraction of in situ cosmogenic carbon-14 in the Tulane University cosmogenic nuclide laboratory. *Nuclear Instruments and Methods in Physics Research Section B: Beam Interactions with Materials and Atoms,* 455**,** 284-292.

Gosse, J. C. & Phillips, F. M. 2001. Terrestrial in situ cosmogenic nuclides: theory and application. *Quaternary Science Reviews,* 20**,** 1475-1560.

Graham, B. L.,Briner, J. P.,Schweinsberg, A. D.,Lifton, N. A. & Bennike, O. 2019. New in situ 14C data indicate the absence of nunataks in west Greenland during the Last Glacial Maximum. *Quaternary Science Reviews,* 225.

Håkansson, L.,Graf, A.,Strasky, S.,Ivy-Ochs, S.,Kubik, P. W.,Hjort, C. & Schlüchter, C. 2016. Cosmogenic 10be-ages from the store koldewey island, ne greenland. *Geografiska Annaler: Series A, Physical Geography,* 89**,** 195-202.

Heyman, J.,Stroeven, A. P.,Harbor, J. M. & Caffee, M. W. 2011. Too young or too old: Evaluating cosmogenic exposure dating based on an analysis of compiled boulder exposure ages. *Earth and Planetary Science Letters,* 302**,** 71-80.

Hill, E. A.,Carr, J. R. & Stokes, C. R. 2017. A Review of Recent Changes in Major Marine-Terminating Outlet Glaciers in Northern Greenland. *Frontiers in Earth Science,* 4.

Hippe, K. 2017. Constraining processes of landscape change with combined in situ cosmogenic 14 C- 10 Be analysis. *Quaternary Science Reviews,* 173**,** 1-19.

Hippe, K.,Kober, F.,Baur, H.,Ruff, M.,Wacker, L. & Wieler, R. 2009. The current performance of the in situ 14C extraction line at ETH. *Quaternary Geochronology,* 4**,** 493-500.

Hippe, K. & Lifton, N. A. 2016. Calculating Isotope Ratios and Nuclide Concentrations for In Situ Cosmogenic 14C Analyses. *Radiocarbon,* 56**,** 1167-1174.

Ivy-Ochs, S. & Kober, F. 2008. Surface exposure dating with cosmogenic nuclides. *Quaternary Science Journal,* 57**,** 179-209.

Jakobsson, M.,Hogan, K. A.,Mayer, L. A.,Mix, A.,Jennings, A.,Stoner, J.,Eriksson, B.,Jerram, K.,Mohammad, R.,Pearce, C.,Reilly, B. & Stranne, C. 2018. The Holocene retreat dynamics and stability of Petermann Glacier in northwest Greenland. *Nat Commun,* 9**,** 2104.

Jennings, A. E.,Andrews, J. T.,Oliver, B.,Walczak, M. & Mix, A. 2019. Retreat of the Smith Sound Ice Stream in the Early Holocene. *Boreas,* 48**,** 825-840.

Jennings, A. E.,Sheldon, C.,Cronin, T. M.,Francus, P.,Stoner, J. & Andrews, J. 2011. The Holocene history of Nares Strait: Transition from Glacial Bay to Arctic-Atlamntic Throughflow. *Oceanography,* 24**,** 27-41.

Kelly, M. A.,Lowell, T. V.,Hall, B. L.,Schaefer, J. M.,Finkel, R. C.,Goehring, B. M.,Alley, R. B. & Denton, G. H. 2008. A 10Be chronology of lateglacial and Holocene mountain glaciation in the Scoresby Sund region, east Greenland: implications for seasonality during lateglacial time. *Quaternary Science Reviews,* 27**,** 2273-2282.

Khan, S. A.,Aschwanden, A.,Bjork, A. A.,Wahr, J.,Kjeldsen, K. K. & Kjaer, K. H. 2015. Greenland ice sheet mass balance: a review. *Rep Prog Phys,* 78**,** 046801.

Kjær, K. H.,Larsen, N. K.,Binder, T.,Bjørk, A. A.,Eisen, O.,Fahnestock, M. A.,Funder, S.,Garde, A. A.,Haack, H.,Helm, V.,Houmark-Nielsen, M.,Kjeldsen, K. K.,Khan, S. A.,Machguth, H.,Mcdonald, I.,Morlighem, M.,Mouginot, J.,Paden, J. D.,Waight, T. E.,Weikusat, C.,Willerslev, E. & Macgreor, J. A. 2018. A large impact crater beneath Hiawatha Glacier in northwest Greenland. *Science Advances,* 4**,** 1-11.

Kolb, J.,Keiding, J. K.,Steenfelt, A.,Secher, K.,Keulen, N.,Rosa, D. & Stensgaard, B. M. 2016. Metallogeny of Greenland. *Ore Geology Reviews,* 78**,** 493-555.

Lal, D. 1991. Cosmic ray labeling of erosion surface: in situ nuclide production rates and erosion models. *Earth and Planetary Science Letters,* 104**,** 424-439.

Larsen, N. K.,Funder, S.,Kjær, K. H.,Kjeldsen, K. K.,Knudsen, M. F. & Linge, H. 2014. Rapid early Holocene ice retreat in West Greenland. *Quaternary Science Reviews,* 92**,** 310-323.

Larsen, N. K.,Levy, L. B.,Carlson, A. E.,Buizert, C.,Olsen, J.,Strunk, A.,Bjork, A. A. & Skov, D. S. 2018. Instability of the Northeast Greenland Ice Stream over the last 45,000 years. *Nat Commun,* 9**,** 1872.

Formatted: Danish

Formatted: Danish

Formatted: Danish

Larsen, N. K.,Levy, L. B.,Strunk, A.,Søndergaard, A. S.,Olsen, J. & Lauridsen, T. L. 2019. Local ice caps in Finderup Land, North Greenland, survived the Holocene Thermal Maximum. *Boreas*.

Larsen, N. K.,Søndergaard, A. S.,Levy, L. B.,Olsen, J.,Strunk, A.,Bjørk, A. A. & Skov, D. S. in press. Contrasting modes of delaciation between fjords and inter-fjord areas in eastern North Greenland.

Lasher, G. E.,Axford, Y.,Mcfarlin, J. M.,Kelly, M. A.,Osterberg, E. C. & Berkelhammer, M. B. 2017. Holocene temperatures and isotopes of precipitation in Northwest Greenland recorded in lacustrine organic materials. *Quaternary Science Reviews,* 170**,** 45-55.

Lecavalier, B. S.,Fisher, D. A.,Milne, G. A.,Vinther, B. M.,Tarasov, L.,Huybrechts, P.,Lacelle, D.,Main, B.,Zheng, J.,Bourgeois, J. & Dyke, A. S. 2017. High Arctic Holocene temperature record from the Agassiz ice cap and Greenland ice sheet evolution. *Proc Natl Acad Sci U S A*.

Levac, E.,Vernal, A. D. & Blake Jr, W. 2001. Sea-surface conditions in northernmost Baffin Bay during the Holocene: palynological evidence. *Journal of Quaternary Science,* 16**,** 353-363.

Lifton, N.,Goehring, B.,Wilson, J.,Kubley, T. & Caffee, M. 2015. Progress in automated extraction and purification of in situ 14C from quartz: Results from the Purdue in situ 14C laboratory. *Nuclear Instruments and Methods in Physics Research Section B: Beam Interactions with Materials and Atoms,* 361**,** 381-386.

Lifton, N. A.,Jull, A. J. T. & Quade, J. 2001. A new extraction technique and production rate estimate for in situ cosmogenic 14C in quartz. *Geochimica et Cosmochimica Acta,* 65**,** 1953-1969.

Livingstone, S. J.,Chu, W.,Ely, J. C. & Kingslake, J. 2017. Paleofluvial and subglacial channel networks beneath Humboldt Glacier, Greenland. *Geology***,** G38860.1.

Lupker, M.,Hippe, K.,Wacker, L.,Steinemann, O.,Tikhomirov, D.,Maden, C.,Haghipour, N. & Synal, H.-A. 2019. In-situ cosmogenic 14C analysis at ETH Zürich: Characterization and performance of a new extraction system. *Nuclear Instruments and Methods in Physics Research Section B: Beam Interactions with Materials and Atoms,* 457**,** 30-36.

Macgregor, J. A.,Fahnestock, M. A.,Catania, G. A.,Aschwanden, A.,Clow, G. D.,Colgan, W. T.,Gogineni, S. P.,Morlighem, M.,Nowicki, S. M. J.,Paden, J. D.,Price, S. F. & Seroussi, H. 2016. A synthesis of the basal thermal state of the Greenland Ice Sheet. *Journal of Geophysical Research: Earth Surface,* 121**,** 1328-1350.

Mason, O. K. 2010. Beach Ridge Geomorphology at Cape Grinnell, northern Greenland:A Less Icy Arctic in the Mid-Holocene. *Danish Journal of Geography,* 110**,** 19.

Mcfarlin, J. M.,Axford, Y.,Osburn, M. R.,Kelly, M. A.,Osterberg, E. C. & Farnsworth, L. B. 2018. Pronounced summer warming in northwest Greenland during the Holocene and Last Interglacial. *Proc Natl Acad Sci U S A,* 115**,** 6357-6362.

Morlighem, M.,Rignot, E.,Mouginot, J.,Seroussi, H. & Larour, E. 2014. Deeply incised submarine glacial valleys beneath the Greenland ice sheet. *Nature Geoscience,* 7**,** 418-422.

Morlighem, M.,Williams, C. N.,Rignot, E.,An, L.,Arndt, J. E.,Bamber, J. L.,Catania, G.,Chauche, N.,Dowdeswell, J. A.,Dorschel, B.,Fenty, I.,Hogan, K.,Howat, I.,Hubbard, A.,Jakobsson, M.,Jordan, T. M.,Kjeldsen, K. K.,Millan, R.,Mayer, L.,Mouginot, J.,Noel, B. P. Y.,O'cofaigh, C.,Palmer, S.,Rysgaard, S.,Seroussi, H.,Siegert, M. J.,Slabon, P.,Straneo, F.,Van Den Broeke, M. R.,Weinrebe, W.,Wood, M. & Zinglersen, K. B. 2017. BedMachine v3: Complete Bed Topography and Ocean Bathymetry Mapping of Greenland From Multibeam Echo Sounding Combined With Mass Conservation. *Geophys Res Lett,* 44**,** 11051-11061.

Mörner, N. A. & Funder, S. V. 1990. C-14 dating of samples collected during the NORDQUA 86 expedition, and notes on the marine reservoir effect. *Meddelelser om Grønland,* 22**,** 57-59.

Mouginot, J.,Rignot, E.,Bjork, A. A.,Van Den Broeke, M.,Millan, R.,Morlighem, M.,Noel, B.,Scheuchl, B. & Wood, M. 2019. Forty-six years of Greenland Ice Sheet mass balance from 1972 to 2018. *Proc Natl Acad Sci U S A,* 116**,** 9239-9244.

Nichols, R., L 1969. Geomorphology of Inglefield Land, North Greenland. *Meddelelser om Grønland,* 188**,** 109.

Nishiizumi, K.,Imamura, M.,Caffee, M. W.,Southon, J. R.,Finkel, R. C. & Mcaninch, J. 2007. Absolute calibration of 10Be AMS standards. *Nuclear Instruments and Methods in Physics Research Section B: Beam Interactions with Materials and Atoms,* 258**,** 403-413.

Noël, B.,Van De Berg, W. J.,Lhermitte, S. & Van Der Broeke, M. R. 2019. Rapid ablation zone expansion amplifies north Greenland mass loss. *Science Advances,* 5.

Olsen, J.,Tikhomirov, D.,Grosen, C.,Heinemeier, J. & Klein, M. 2016. Radiocarbon Analysis on the New AARAMS 1MV Tandetron. *Radiocarbon,* 59**,** 905-913.

Ramsey, B. C. 2009. Bayesian Analysis of Radiocarbon Dates. *Radiocarbon,* 51**,** 337-360.

Reilly, B. T.,Stoner, J. S.,Mix, A. C.,Walczak, M. H.,Jennings, A.,Jakobsson, M.,Dyke, L.,Glueder, A.,Nicholls, K.,Hogan, K. A.,Mayer, L. A.,Hatfield, R. G.,Albert, S.,Marcott, S.,Fallon, S. & Cheseby, M. 2019. Holocene break-up and reestablishment of the Petermann Ice Tongue, Northwest Greenland. *Quaternary Science Reviews,* 218**,** 322-342.

Reimer, J. P.,Bard, E.,Bayliss, A.,Beck, J. W.,Blackwell, P. G.,Ramsey, C. B.,Buck, C. E.,Cheng, H.,Edwards, R. L.,Friedrich, M.,Grootes, P. M.,Guilderson, T. P.,Haflidason, H.,Hajdas, I.,Hatté, C.,Heaton, T. J.,Hoffmann, D. L.,Hogg, A. G.,Hughen, K. A.,Kaiser, K. F.,Kromer, B.,Manning, S. W.,Niu, M.,Reimer, R. W.,Richards, D. A.,Scott, E. M.,Southon, J. R.,Staff, R.

Formatted: Danish

Formatted: Danish

Formatted: Danish

Formatted: Danish

Formatted: Danish

A.,Turney, C. S. M. & Van Der Plicht, J. 2013. Intcal13 and Marine13 radiocarbon age calibration curves 0-50,000 years cal BP. *Radiocarbon,* 4**,** 1869-1887.

Reusche, M. M.,Marcott, S. A.,Ceperley, E. G.,Barth, A. M.,Brook, E. J.,Mix, A. C. & Caffee, M. W. 2018. Early to Late Holocene Surface Exposure Ages From Two Marine-Terminating Outlet Glaciers in Northwest Greenland. *Geophysical Research Letters,* 45**,** 7028-7039.

Rignot, E. & Kanagaratnam, P. 2006. Changes in the Velocity Structure of the Greenland Ice Sheet. *Science,* 311**,** 986-990.

Sinclair, G.,Carlson, A. E.,Mix, A. C.,Lecavalier, B. S.,Milne, G.,Mathias, A.,Buizert, C. & Deconto, R. 2016. Diachronous retreat of the Greenland ice sheet during the last deglaciation. *Quaternary Science Reviews,* 145**,** 243-258.

Skov, D. S.,Egholm, D. L.,Larsen, N. K.,Jansen, J. D.,Knudsen, M. F.,Jacobsen, B. H.,Olsen, J. & Andersen, J. L. 2020. Constraints from cosmogenic nuclides on the glaciation and erosion history of Dove Bugt, northeast Greenland. *GSA Bulletin*.

Søndergaard, A. S.,Larsen, N. K.,Lecavalier, B. S.,Olsen, J.,Fitzpatrick, N. P.,Kjær, K. H. & Khan, S. A. 2020. Early Holocene collapse of marine-based ice in northwest Greenland triggered by atmospheric warming. *Quaternary Science Reviews,* 239.

Søndergaard, A. S.,Larsen, N. K.,Olsen, J.,Strunk, A. & Woodroffe, S. 2019. Glacial history of the Greenland Ice Sheet and a local ice cap in Qaanaaq, northwest Greenland. *Journal of Quaternary Science,* 34**,** 536-547.

Stone, J. O. 2000. Air pressure and cosmogenic isotope production. *Journal of Geophysical Research: Solid Earth,* 105**,** 23753-23759.

Synal, H.-A.,Stocker, M. & Suter, M. 2007. MICADAS: A new compact radiocarbon AMS system. *Nuclear Instruments and Methods in Physics Research Section B: Beam Interactions with Materials and Atoms,* 259**,** 7-13.

Tedrow, J. C. F. 1970. Soil investigation in Inglefield Land, Greenland. *Meddelelser om Grønland,* 188.

Wacker, L.,Bonani, G.,Friedrich, M.,Hajdas, I.,Kromer, B.,Němec, M.,Ruff, M.,Suter, M.,Synal, H. A. & Vockenhuber, C. 2010. MICADAS: Routine and High-Precision Radiocarbon Dating. *Radiocarbon,* 52**,** 252-262.

Young, N. E.,Briner, J. P.,Miller, G. H.,Lesnek, A. J.,Crump, S. E.,Thomas, E. K.,Pendleton, S. L.,Cuzzone, J.,Lamp, J.,Zimmerman, S.,Caffee, M. & Schaefer, J. M. 2020. Deglaciation of the Greenland and Laurentide ice sheets interrupted by glacier advance during abrupt coolings. *Quaternary Science Reviews,* 229.

Young, N. E.,Briner, J. P.,Rood, D. H.,Finkel, R. C.,Corbett, L. B. & Bierman, P. R. 2012. Age of the Fjord Stade moraines in the Disko Bugt region, western Greenland, and the 9.3 and 8.2 ka cooling events. *Quaternary Science Reviews,* 60**,** 76-90.

Young, N. E.,Lamp, J.,Koffman, T.,Briner, J. P.,Schaefer, J.,Gjermundsen, E. F.,Linge, H.,Zimmerman, S.,Guilderson, T. P.,Fabel, D. & Hormes, A. 2018. Deglaciation of coastal south-western Spitsbergen dated with in situ cosmogenic 10Be and 14C measurements. *Journal of Quaternary Science,* 33**,** 763-776.

Young, N. E.,Schaefer, J. M.,Briner, J. P. & Goehring, B. M. 2013. A 10Be production-rate calibration for the Arctic. *Journal of Quaternary Science,* 28**,** 515-526.

Young, N. E.,Schaefer, J. M.,Goehring, B.,Lifton, N.,Schimmelpfennig, I. & Briner, J. P. 2014. West Greenland and globalin situ14C production-rate calibrations. *Journal of Quaternary Science,* 29**,** 401-406.

Formatted: Danish

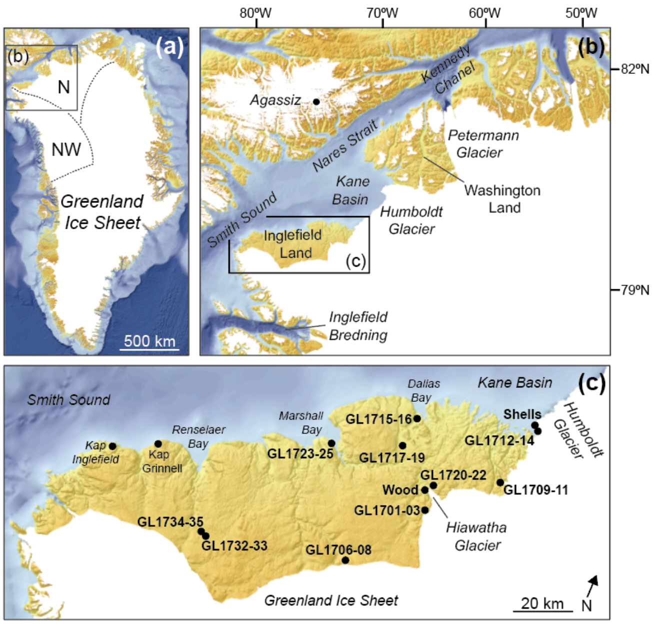

Figure 1: Location of the study area in Greenland (a), with marked northwest (NW) and north (N) Greenland extent and places mentioned in the text (b). (c) shows Inglefield Land with places discussed in the text. Black dots denote sample locations for wood fragments in front of the Hiawatha Glacier, molluscs at the margin of the Humboldt Glacier and boulder samples (GL17XX) collected throughout the study area.

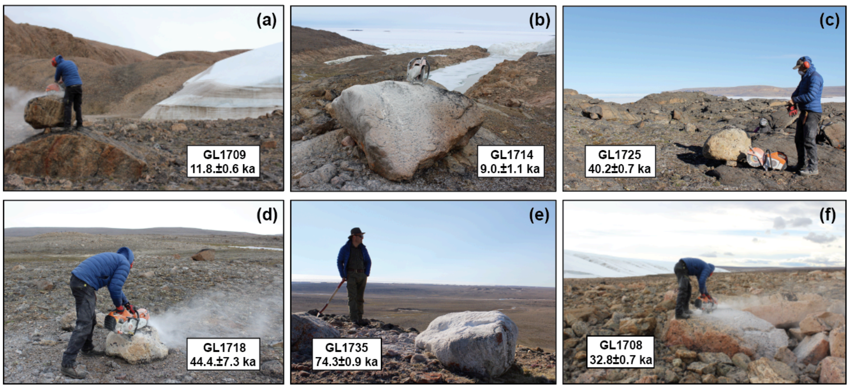

Figure 2: Boulders sampled for ^{10}Be exposure dating in Inglefield Land ((a)-(f)), as well as resulting ages. (a), (f) show boulders sampled close to the present-day ice margin. (b) is a boulder sampled next to the Humboldt Glacier. (c), (d) show boulders samples close to the outer coast. (e) shows a boulder sampled on a moraine in the western part of the study area.

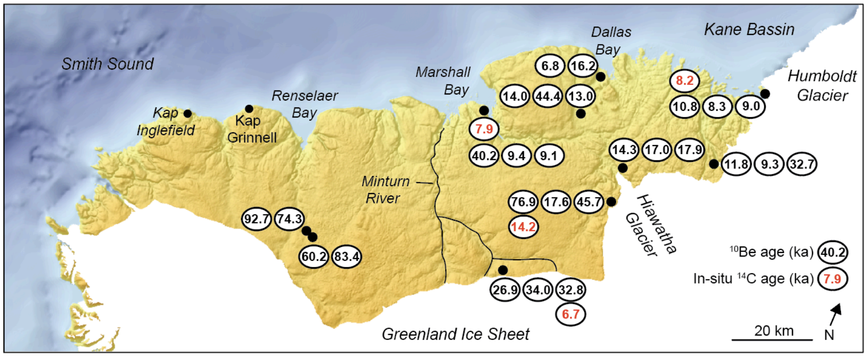

Figure 3: Map of Inglefield Land, north Greenland. Black dots denote sample locations for boulder samples and their resulting ^{10}Be and in-situ ^{14}C exposure ages given in ka. ^{10}Be age uncertainties range between 0.3 ka and 7.3 ka with an average of 1.4 ka and ^{14}C age uncertainties range between 0.3 ka and 0.5 ka with an average of 0.4 ka.

Formatted: Superscript

Formatted: Superscript

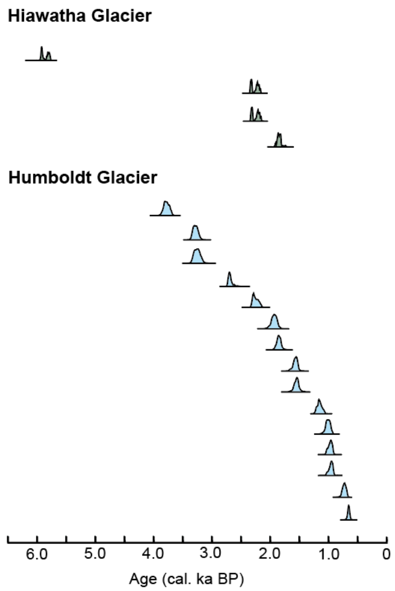

Figure 4: Radiocarbon age probability plots of wood fragments collected in front of the Hiawatha Glacier (green) and reworked marine molluscs collected at the margin of Humboldt Glacier (blue). Each plot represents the age of a single wood fragment or mollusc shell and its calibrated age probability distribution.

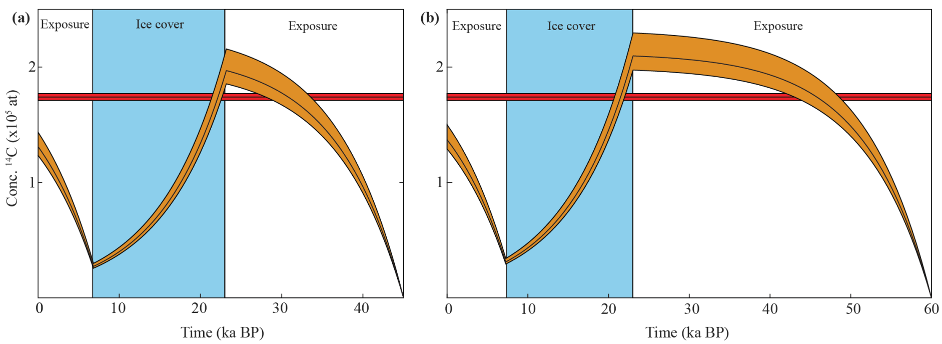

Figure 5: Modelled exposure scenario for boulder sample GL1701. The red line shows the measured in-situ ^{14}C concentration in the sample and the orange line is the nuclide concentration build up and decay during periods of exposure and ice cover. (a) shows exposure from 45 to 23 ka and again from 6.7 ka until present and ice cover in between. (b) shows exposure from 60 to 23 ka and again from 6.7 ka until present and ice cover in between.

Deleted: from

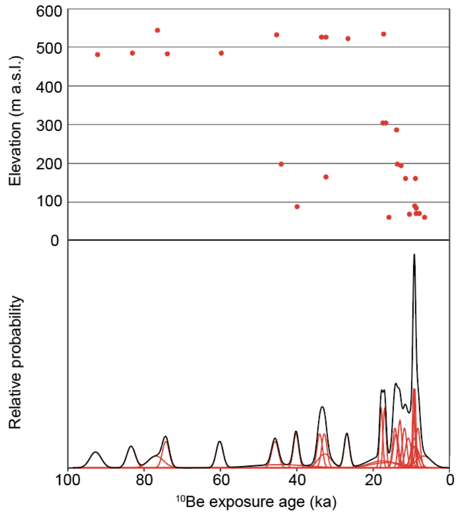

Figure 6: ^{10}Be ages from boulders sampled at various elevations in Inglefield Land, north Greenland. The top panel shows ^{10}Be ages plotted against elevation of the sample sites. Each red dot represents the ^{10}Be age of an individual boulder and its associated elevation. The bottom panel shows the relative probability distribution of the boulder ages with their 1σ analytical uncertainty (red lines) and the cumulated probability plot of all ^{10}Be ages (black line).

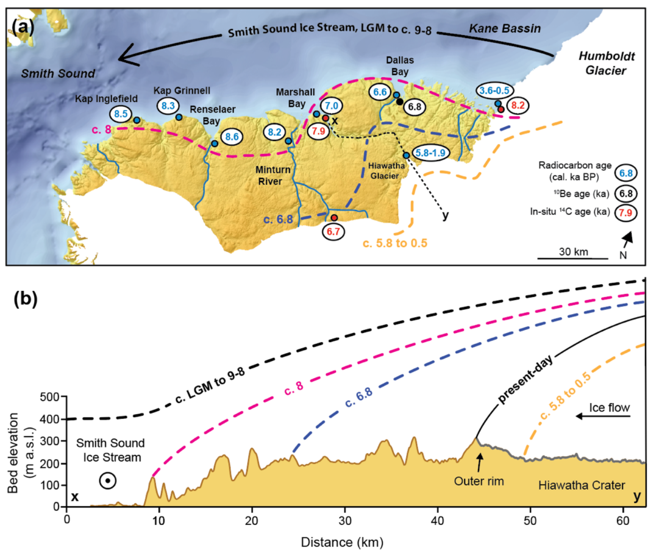

Figure 7: Deglaciation in Inglefield Land. (a) shows ages believed to constrain the deglaciation in the area. In-situ ^{14}C ages and radiocarbon ages at Humboldt Glacier and Hiawatha Glacier are from this study. Radiocarbon ages at the coast are from Nichols (1969), Blake et al. (1992) and Mason (2010). (b) shows the Holocene deglaciation pattern in Inglefield Land inferred from this study across the transect (x-y) seen in (a).

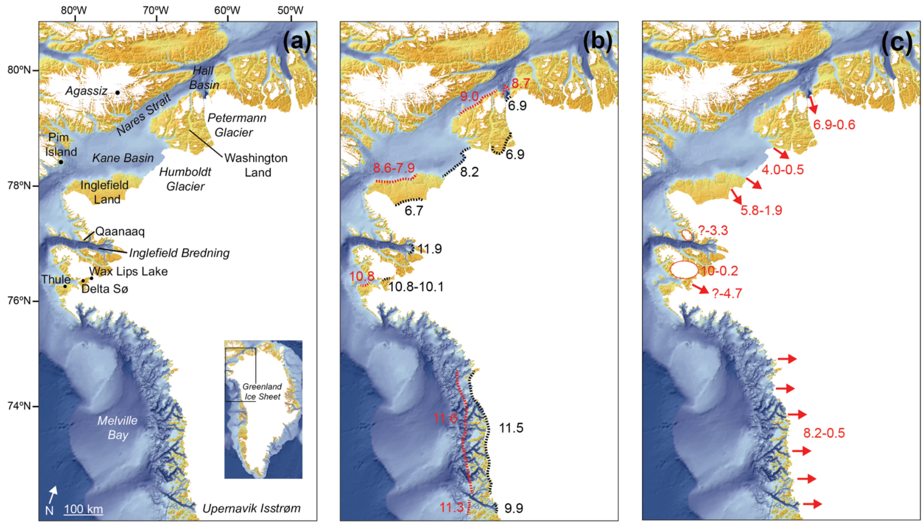

Figure 8: Age constraints (in ka) of the Holocene ice extent at the outer coast, present-day ice margin and for the period when the GrIS was smaller than present. (a) shows localities in northwest and north Greenland. (b) shows the initial Holocene deglaciation of the GrIS towards the outer coast (red) (Corbett et al., 2013; Corbett et al., 2015; Jakobsson et al., 2018; Ceperley et al., 2020; Søndergaard et al., 2020) and following retreat towards the present-day ice margin (black) (Briner et al., 2013; McFarlin et al., 2018; Reusche et al., 2018; Axford et al., 2019; Reilly et al., 2019; Søndergaard et al., 2019; Ceperley et al., 2020; Søndergaard et al., 2020). (c) shows the period when the GrIS and its outlets (arrows) and local ice caps (circles) were smaller than the present-day extent (Bennike, 2002; Bennike, 2008; Briner et al., 2014; Farnsworth et al., 2018; Axford et al., 2019; Reilly et al., 2019; Søndergaard et al., 2019; Søndergaard et al., 2020). A question mark means that the upper limit of restricted ice extent has not been constrained.

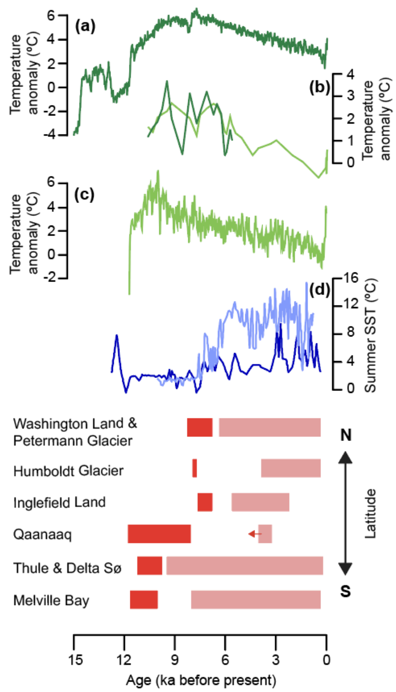

Figure 9: Ice extent and climate fluctuations for north and northwest Greenland during the last 15 ka. (a) mean annual temperature anomalies, northwest Greenland (Buizert et al., 2018). (b) July air temperature anomalies at Delta Sø, northwest Greenland, using two different training sets and transfer functions, FOR15 (light green) and FRA06 (dark green) (Axford et al., 2019). (c) Agassiz $\delta^{18}O$ temperature reconstruction (Lecavalier et al., 2017). (d) Reconstructed west Greenland sea surface temperatures from Gibb et al. (2015) (dark blue) and Ouellet-Bernier et al. (2014) (light blue). The lower panel shows the inferred ice extent in north and northwest Greenland from Melville Bay in the south to Washington Land in the north (for references, see text). Dark red bars denote known periods of deglaciation from the outer coast towards the present-day ice margin and bright red bars denote periods of smaller than present-day extent. Arrows indicate the lack of an upper or lower constraint.

Table 1: Sample collection, ^{10}Be isotopic information and resulting exposure ages for 25 boulder and two pebble samples from Inglefield Land, north Greenland.

Sample name	Sample type	Elevation (m a.s.l.)	Latitude (ºN)	Longitude (ºW)	Sample thickness (cm)	Shielding correction	Quartz (g)	Carrier added (g)[a]	Sample ^{10}Be/^{9}Be ratio (10^{-14})	Blank ^{10}Be/^{9}Be ratio (10^{-14})	^{10}Be conc. (atoms/g)	^{10}Be unc. (atoms/g)	^{10}Be age (ka)[b]
GL1701	Boulder	542	78.76	-67.01	5.8	0.9999	40.006	0.739	130.9±2.8	0.3±0.08	529068	13417	76.9±2.0
GL1702	Boulder	533	78.76	-67.01	5.2	0.9997	40.046	0.751	30.0±5.7	0.3±0.08	122306	23513	17.6±3.4
GL1703	Boulder	530	78.76	-67.02	5.7	0.9994	40.084	0.762	75.4±1.1	0.3±0.08	312981	6183	45.7±0.9
GL1706	Boulder	521	78.51	-67.94	5.3	0.9997	40.176	0.751	45.3±1.0	0.3±0.08	184398	4623	26.9±0.7
GL1707	Boulder	524	78.51	-67.94	5.7	0.9997	40.428	0.756	57.0±0.9	0.3±0.08	232494	4811	34.0±0.7
GL1708	Boulder	524	78.51	-67.94	5.4	0.9998	40.071	0.752	55.0±1.0	0.3±0.08	225228	5069	32.8±0.7
GL1709	Boulder	159	78.94	-67.02	5.4	0.9952	40.043	0.602	17.2±0.8	0.3±0.08	55336	2595	11.8±0.6
GL1710	Boulder	159	78.94	-67.02	5.3	0.9963	40.050	0.603	13.7±1.1	0.3±0.08	43909	3758	9.3±0.8
GL1711	Boulder	163	78.94	-66.02	4.8	0.9950	40.065	0.205	47.6±2.5	0.02±0.01	154443	8090	32.7±1.7
GL1712	Boulder	65	79.14	-65.81	5.6	0.9998	34.035	0.206	11.9±0.9	0.02±0.01	45662	3555	10.8±0.8
GL1713	Boulder	67	79.14	-65.81	5.3	0.9998	40.261	0.214	10.5±0.7	0.02±0.01	35421	2451	8.3±0.6
GL1714	Boulder	67	79.14	-65.81	6.0	0.9999	40.088	0.214	11.3±1.4	0.02±0.01	38144	4846	9.0±1.1
GL1715	Pebbles	58	79.03	-67.80	0.7	0.9999	40.235	0.205	9.2±2.6	0.02±0.01	29660	8520	6.8±2.0
GL1716	Pebbles	58	79.03	-67.80	2.2	0.9999	40.196	0.212	20.9±5.6	0.02±0.01	69622	18782	16.2±4.4
GL1717	Boulder	195	78.93	-67.82	6.0	0.9981	40.114	0.443	9.8±0.5	0.02±0.01	68250	3283	14.0±0.7
GL1718	Boulder	195	78.93	-67.82	5.7	0.9981	40.012	0.210	64.8±10.5	0.02±0.01	215174	34752	44.4±7.3
GL1719	Boulder	191	78.93	-67.82	3.9	0.9997	40.031	0.207	19.7±0.8	0.02±0.01	64477	2743	13.0±0.5
GL1720	Boulder	284	78.84	-67.09	3.3	0.9993	40.159	0.215	23.3±0.9	0.02±0.01	78937	3097	14.3±0.6
GL1721	Boulder	302	78.84	-67.09	3.9	0.9983	40.038	0.208	28.9±0.7	0.2±0.05	94273	2377	17.0±0.4
GL1722	Boulder	301	78.84	-67.09	4.5	0.9983	40.016	0.205	30.3±0.7	0.2±0.05	99077	2296	17.9±0.4
GL1723	Boulder	87	78.85	-68.89	4.7	0.9989	40.039	0.203	12.8±0.5	0.2±0.05	40899	1501	9.4±0.3
GL1724	Boulder	82	78.85	-68.89	5.6	0.9992	40.024	0.206	12.3±0.4	0.2±0.05	39377	1370	9.1±0.3
GL1725	Boulder	86	78.85	-68.89	5.7	0.9991	40.006	0.203	53.8±0.9	0.2±0.05	172559	3088	40.2±0.7
GL1732	Boulder	483	78.41	-70.32	4.6	1	40.059	0.201	124.6±1.5	0.2±0.05	396868	5565	60.2±0.9
GL1733	Boulder	483	78.41	-70.32	5.6	1	39.648	0.201	168.7±1.9	0.2±0.05	542019	7114	83.4±1.1
GL1734	Boulder	480	78.41	-70.33	4.9	1	34.450	0.204	158.9±2.2	0.2±0.05	602773	9256	92.7±1.5
GL1735	Boulder	482	78.41	-70.33	5.3	1	40.007	0.208	147.0±1.5	0.2±0.05	484687	5982	74.3±0.9

[a] Carrier *Phe1602* (328.2±3.7 µg ^{9}Be/g) was used for preparation of sample GL1701-GL1703 and GL1706-GL1710. All other samples were prepared using carrier *Phe1603* (949.4±6.2 µg ^{9}Be/g).

[b] ^{10}Be ages were calculated using the online exposure age calculator formerly known as the CRONUS-Earth online exposure calculator v.3 (Balco et al., 2008), the Baffin Bay production rate (Young et al., 2013), and the St scaling scheme (Lal, 1991; Stone, 2000) under standard atmosphere. A rock density of 2.65 g cm^{-3} was used and we assumed zero erosion. Samples were normalized to the Beryllium standard ICN-01-5-4, with a ^{10}Be/^{9}Be value of 2.851 x 10^{-12} (Nishiizumi et al., 2007) and blank corrected. ^{10}Be age uncertainties are reported as the 1σ internal uncertainty.

Table 2: Sample collection, ^{14}C isotopic information and resulting exposure ages for 4 boulders from Inglefield Land, north Greenland.

Sample name	Elevation (m a.s.l.)	Latitude (ºN)	Longitude (ºW)	Shielding correction	Quartz (g)	CO_2 yield (µg)	$F^{14}C$	$\delta^{13}C$ (‰)	$^{14}C/^{12}C_{total}$ (10^{-14})	^{14}C atoms blank corrected (10^5) [b]	^{14}C (10^5 at g^{-1})	^{14}C exposure age (ka) [c]
GL1701	542	78.76	67.01	0.9999	3.9552	22.93	0.550	-10.1	65.0±0.71	6.88±0.10	1.74±0.03	14.2±0.5
GL1708	524	78.51	67.94	0.9998	3.9036	76.28	0.114	-10.8	13.4±0.25	4.54±0.11	1.16±0.03	6.7±0.3
GL1712	65	79.14	65.81	0.9998	3.9156	80.01	0.083	-12.9	9.70±0.23	3.30±0.11	0.84±0.03	8.2±0.5
GL1725	86	78.85	68.89	0.9991	3.8113	77.42	0.083	-11.6	9.77±0.23	3.20±0.10	0.84±0.03	7.9±0.4

[a] Normalized to $\delta^{13}C$ of -25‰ VPDB and AD 1950

[b] All samples were blank corrected (0.589±0.052 10^5 ^{14}C atoms)

[c] ^{14}C ages were calculated using the online exposure age calculator formerly known as the CRONUS-Earth online exposure calculator v.3 (Balco et al., 2008), the west Greenland production rate (Young et al., 2014), and the Lm scaling scheme (Lal, 1991; Stone, 2000) under standard atmosphere. A rock density of 2.65 g cm^{-3} was used and we assumed zero erosion. ^{14}C age uncertainties are reported as the 1σ analytical uncertainty.

Table 3: Sample collection information, radiocarbon ages and calibrated ages for marine molluscs collected at the margin of the Humboldt Glacier and wood fragments collected in front of the Hiawatha Glacier, north Greenland.

Lab ID	Sample material	Latitude (ºN)	Longitude (ºW)	Elevation (m a.s.l.)	Age (^{14}C yr BP)	Age (95 % range) (cal. yr BP)[a]	Mean age (cal. yr BP ±2 σ)[a]
AAR-27511	*Mya truncata*				2006±24	1321-1494	1400±44
AAR-27512	*Mya truncata*				1589±22	920-1050	983±35
AAR-27513	*Mya truncata*				3387±34	2937-3166	3052±60
AAR-27514	*Mya truncata*				2899±27	2345-2606	2466±70
AAR-27515	*Mya truncata*				3831±26	3501-3684	3593±44
AAR-27516	*Mya truncata*				1093±20	499-605	542±28
AAR-27517	*Mya truncata*				1415±23	736-891	812±41
AAR-27518	*Hiatella arctica*	79.143	65.797	90	3413±25	2984-3181	3087±50
AAR-27519	*Hiatella arctica*				1988±28	1299-1474	1379±45
AAR-27520	*Hiatella arctica*				1195±23	553-662	613±30
AAR-27521	*Hiatella arctica*				2580±25	1979-2148	2066±45
AAR-27522	*Hiatella arctica*				1428±23	749-900	825±39
AAR-27523	*Hiatella arctica*				2318±33	1698-1884	1793±49
AAR-27524	*Hiatella arctica*				2248±22	1666-1865	1761±49
AAR-27525	*Astarte borealis*				1466±25	783-922	857±38
471815	Wood				2260±30	2158-2346	2256±59
471816	Wood	78.830	67.133	193	1910±30	1741-1929	1854±37
471817	Wood				2260±30	2158-2346	2256±59
471818	Wood				5120±30	5751-5930	5846±59

[a] Radiocarbon ages were calibrated using OxCal v4.3 (Ramsey, 2009). The Marine13 calibration curve (Reimer et al., 2013) and a marine reservoir effect of 550 ^{14}C yr (ΔR=150) (Mörner and Funder, 1990) were used for calibrating sample AAR-27511 to AAR-27525. For sample 471815-471818, the Intcall13 curve was used for calibration (Reimer et al., 2013).